TURUN YLIOPISTON JULKAISUJA
ANNALES UNIVERSITATIS TURKUENSIS

*SARJA - SER. A I OSA - TOM. 385*

ASTRONOMICA - CHEMICA - PHYSICA - MATHEMATICA

# SURFACE STUDIES OF THIOLATE ADSORBATES ON SOME METALS

by

Taina Laiho

TURUN YLIOPISTO
Turku 2008

From the Laboratory of Materials Science
Department of Physics and Astronomy
University of Turku
Turku, Finland

*Supervised by*

Docent Jarkko Leiro
Laboratory of Materials Science
Department of Physics and Astronomy
University of Turku
Turku, Finland

*Reviewed by*

Professor Anne Borg
Department of Physics
Norwegian University of Science and Technology (NTNU)
Trondheim, Norway

and

Professor Giorgio Contini
Istituto di Struttura della Materia (CNR-ISM)
Physics department, Tor Vergata University
Rome, Italy

ISBN 978-951-29-3740-0 (PRINT)
ISBN 978-951-29-3741-7 (PDF)
ISSN 0082-7002
Painosalama Oy – Turku, Finland 2008

# Preface

This thesis is based on work carried out at the Laboratory of Materials Science, University of Turku.

I am grateful to and thank my supervisor, Docent Jarkko Leiro, for his support and guidance. I have had many interesting scientific and other discussions with Jarkko and he encouraged me to complete this thesis. I also thank Professor Edwin Kukk who arranged the financing for me to complete these studies.

Prof. Jukka Lukkari and others from the Department of Chemistry are acknowledged for fruitful cooperation.

I want to thank all my friends and colleagues, past and present, from the Laboratory of Materials Science. Special thanks to Sari, Riitta and Robert with whom I have been able to talk about everything – scientific problems and personal feelings.

Prof. Anne Borg and Prof. Giorgio Contini are acknowledged for critically reviewing this thesis, and Dr. Michael Nelson is acknowledged for correcting the language.

The work at MAX-lab was financially supported by the European Community Access to Research Infrastructure Action of the Improving Human Potential Programme (ARI), which is acknowledged.

Thanks to Seija and Harri Mela for encouraging me during the writing process.

And finally, I thank my parents Mirja and Ilkka Laiho and my brother Tero. I also want to thank Reetta and Olavi Rautio. Special thanks to Petri, Veera and Oona for all the experiences we have lived through together and for giving me something else to think about than just my work and science.

Turku, November 2008

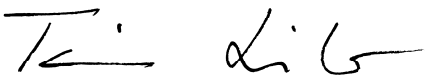

Taina Laiho

# Table of contents

# Abbreviations

| | |
|---|---|
| AA | absolute alcohol |
| AFM | atomic force microscopy |
| BE | binding energy |
| BL | beamline |
| CPE | constant phase element |
| $C_{12}SH$ | $CH_3(CH_2)_{11}SH$ |
| $C_{12}SSO_3Na$ | $CH_3(CH_2)_{11}SSO_3Na$ |
| DS | Doniach-Šunjić peak shape |
| ESCA | electron spectroscopy for chemical analysis |
| FT-IR | fourier transform infrared spectroscopy |
| FWHM | full width at half-maximum |
| HR-XPS | synchrotron radiation excited high resolution photoelectron spectroscopy |
| IMFP | inelastic mean free path |
| LB | Langmuir-Blodgett |
| LEED | low energy electron diffraction |
| LINAC | linear accelerator |
| M-H | deprotonated $CH_3(CH_2)_{11}SH$ |
| Me | metal atom |
| MED | mean escape depth |
| PDMS | poly(dimethylsiloxane) |
| R | hydrocarbon group |
| SAM | self-assembled monolayer |
| SIMS | secondary ion mass spectrometry |
| STM | scanning tunneling microscopy |
| ToF-SIMS | time-of-flight secondary ion mass spectrometry |
| UHV | ultra high vacuum |
| XPS | X-ray photoelectron spectroscopy |

# Abstract

The results and discussions in this thesis are based on my studies about self-assembled thiol layers on gold, platinum, silver and copper surfaces. These kinds of layers are two-dimensional, one molecule thick and covalently organized at the surface. They are an easy way to modify surface properties. Self-assembly is today an intensive research field because of the promise it holds for producing new technology at nanoscale, the scale of atoms and molecules. These kinds of films have applications for example, in the fields of physics, biology, engineering, chemistry and computer science.

Compared to the extensive literature concerning self-assembled monolayers (SAMs) on gold, little is known about the structure and properties of thiol-based SAMs on other metals. In this thesis I have focused on thiol layers on gold, platinum, silver and copper substrates. These studies can be regarded as a basic study of SAMs. Nevertheless, an understanding of the physical and chemical nature of SAMs allows the correlation between atomic structure and macroscopic properties. The results can be used as a starting point for many practical applications.

X-ray photoelectron spectroscopy (XPS) and synchrotron radiation excited high resolution photoelectron spectroscopy (HR-XPS) together with time-of-flight secondary ion mass spectrometry (ToF-SIMS) were applied to investigate thin organic films formed by the spontaneous adsorption of molecules on metal surfaces. Photoelectron spectroscopy was the main method used in these studies. In photoelectron spectroscopy, the sample is irradiated with photons and emitted photoelectrons are energy-analyzed. The obtained spectra give information about the atomic composition of the surface and about the chemical state of the detected elements. It is widely used in the study of thin layers and is a very powerful tool for this purpose. Some XPS results were complemented with ToF-SIMS measurements. It provides information on the chemical composition and molecular structure of the samples.

Thiol (1-Dodecanethiol, $CH_3(CH_2)_{11}SH$) solution was used to create SAMs on metal substrates. Uniform layers were formed on most of the studied metal surfaces. On platinum, surface aligned molecules were also detected in investigations by XPS and ToF-SIMS. The influence of radiation on the layer structure was studied, leading to the conclusion that parts of the hydrocarbon chains break off due to radiation and the rest of the layer is deformed. The results obtained showed differences depending on the substrate material. The influence of oxygen on layer formation was also studied. Thiol molecules were found to replace some of the oxygen from the metal surfaces.

# List of publications

The content of this thesis is based on the following published papers. The author was also responsible for performing all the XPS measurements and most of the sample preparations. The papers are referred to by their Roman numerals in the text.

I T. Laiho, J.A. Leiro and J. Lukkari:
XPS study of irradiation damage and different metal-sulfur bonds in dodecanethiol monolayers on gold and platinum surfaces.
*Applied Surface Science* **2003**, *212-213*, 525-529.

II T. Laiho, J.A. Leiro, S. Mattila, M. Heinonen and J. Lukkari:
Photoelectron spectroscopy study of irradiation damage and metal-sulfur bonds of thiol on silver and copper surfaces.
*Journal of Electron Spectroscopy and Related Phenomena* **2005**, *142*, 105-112.

III T. Laiho, J. Lukkari, M. Meretoja, K. Laajalehto, J. Kankare and J.A. Leiro:
Chemisorption of alkyl thiols and S-alkyl thiosulfates on Pt(111) and polycrystalline platinum surfaces.
*Surface Science* **2005**, *584*, 83–89.

IV T. Laiho and J.A. Leiro:
Influence of initial oxygen on the formation of thiol layers.
*Applied Surface Science* **2006**, *252*, 6304–6312.

V T. Laiho and J.A. Leiro:
ToF-SIMS study of 1-dodecanethiol adsorption on Au, Ag, Cu and Pt surfaces.
*Surface and Interface Analysis* **2008**, *40*, 51-59.

A list of other published articles, concerning XPS studies of sulfur-containing species and of thin organic layers, where I am a co-author. These publications are related to this work, but were not included in the thesis.

K. Laajalehto, I. Kartio, T. Kaurila, T. Laiho and E. Suoninen:
Investigation of copper sulfide surfaces using synchrotron radiation excited photoemission spectroscopy,
Mathieu, H.J., Reihl, B. and Briggs, D. (Ed.), *Proc. of 6th European Conference on Applications of Surface and Interface Analysis (ECASIA 95)*, pp. 717-720, John Wiley & Sons, Chichester, England (**1996**).

I. Kartio, G. Wittstock, K. Laajalehto, D. Hirsch, J. Simola, T. Laiho, R. Szargan and E. Suoninen:
Detection of elemental sulfur on galena oxidized in acidic solution.
*International Journal of Mineral Processing* **1997**, *51*, 293-301.

K. Laajalehto, J. Leppinen, I. Kartio and T. Laiho:
XPS and FTIR study of the influence of electrode potential on activation of pyrite by copper or lead.
*Colloids and Surfaces A* **1999**, *154*, 193-199.

K. Laajalehto, I. Kartio, M. Heinonen and T. Laiho:
Temperature controlled photoelectron spectroscopic investigation of volatile species on PbS (100) surface.
*Japanese Journal of Applied Physics* **1999**, *38-1*, 265-268.

J. Lukkari, M. Salomaki, T. Ääritalo, K. Loikas, T. Laiho and J. Kankare:
Preparation of multilayers containing conjugated thiophene-based polyelectrolytes. Layer-by-layer assembly and viscoelastic properties.
*Langmuir* **2002**, *18(22)*, 8496-8502.

J.A. Leiro, M.H. Heinonen, T. Laiho and I.G. Batirev:
Core-level XPS spectra of fullerene, highly oriented pyrolitic graphite, and glassy carbon.
*Journal of Electron Spectroscopy and Related Phenomena* **2003**, *128(2-3)*, 205-213.

A. Viinikanoja, J. Lukkari, T. Ääritalo, T. Laiho and J. Kankare:
Phosphonic acid derivatized polythiophene: a building block for metal phosphonate and polyelectrolyte multilayers.
*Langmuir* **2003**, *19(7)*, 2768-2775.

J.P. Matinlinna, K. Laajalehto, T. Laiho, I. Kangasniemi, L.V.J. Lassila and P.K. Vallittu:
Surface analysis of Co-Cr-Mo-alloy and Ti substrates silanized with trialkoxysilanes and silane mixtures.
*Surface and Interface Analysis* **2004**, *36(3)*, 246-253.

M. Salomäki, T. Laiho and J. Kankare:
Counteranion-controlled properties of polyelectrolyte multilayers.
*Macromolecules* **2004**, *37(25)*, 9585-9590.

H. Paloniemi, T. Ääritalo, T. Laiho, H. Liuke, N. Kocharova, K. Haapakka, F. Terzi, R. Seeber, J. Lukkari:
Water-soluble full-length single-wall carbon nanotube polyelectrolytes: preparation and characterization.
*Journal of Physical Chemistry B* **2005**, *109(18)*, 8634-8642.

S. Mattila, J.A. Leiro, M. Heinonen and T. Laiho:
Core level spectroscopy of $MoS_2$.
*Surface Science* **2006**, *600(24)*, 5168-5175.

# 1. Introduction

Self-assembled monolayers (SAMs) of thiol molecules were chosen to be the subject of these studies. During recent decades sulfur-containing self-assembled organic monolayers have been found to be important agents for altering the properties of solid surfaces, and have shown considerable technological potential. They provide an easy method to create high-quality organic thin films with tailored electronic and chemical properties. This gives possibilities to use them in many kinds of applications. Despite intense studies concerning thiol monolayers many important details are still under investigation in research groups world-wide.

Traditionally, sulfur-containing molecules on the surfaces of metals and metal oxides have received considerable attention due to the negative effects of sulfur in the chemical industry. In industrial catalytic processes the sulfur impurities rapidly deactivate or poison most metal/oxide catalysts.[1,2] As a result of ongoing research, sulfur-containing molecules are receiving more positive attention. Due to their relevance for numerous applications SAMs have become a highly active research field internationally. Numerous articles have been written and patents have been applied concerning surfaces modified by SAMs. Accelerating the development of applications based on thin films will depend on the ability of researchers to more accurately characterize the physical and chemical properties of these systems.

In this thesis, X-ray photoelectron spectroscopy (XPS), synchrotron radiation excited high resolution photoelectron spectroscopy and time-of-flight secondary ion mass spectrometry (ToF-SIMS) were applied to investigate thin organic films formed by the adsorption of thiol on metal surfaces. The XPS method is widely used to analyze thin organic layers. The usefulness of XPS as an analysis tool for these kinds of films is based on an understanding of the advantages and also the disadvantages of the method.

# 2. Self-assembled monolayers

Self-assembled monolayers (SAMs) are spontaneously formed layers that can be used to modify the chemical and physical properties of surfaces. By modifying the molecule one can change surface properties.

There are a number of reported surface active compounds that form SAMs. Organosulfur compounds are often used to form monolayers on transition metal surfaces, and chlorosilanes (-Si-Cl) and alkoxysilanes (-Si-OR) can also be used. Some of the most commonly used molecules belong to the alkyls bearing mercapto (-SH) group, thiols. Long-chain thiols form well-organized, closely packed and stable monolayers on different surfaces. Generally, the molecules that are used in self-assembly processes consist of a surface-active headgroup, which binds to the substrate surface by chemisorption, and a molecular body, which stands away from the surface. Certain properties of the monolayer can be adjusted by changing the chemical nature of the terminal groups. Functionalized alkanethiolate SAMs are important both for the engineering of surface properties and for further chemical reactions. Flexibility, well-defined composition and thickness together with a simple preparation make these organic thin films excellent systems to control interactions on the metal/environment interface.[3]

## 2.1. Formation of self-assembled monolayers

Langmuir-Blodgett (LB) was the first technique to provide the practical capability to construct ordered molecular assemblies. This method is based on the idea that amphiphilic molecules form monolayers at water-air interfaces. When a solid substrate is moved through the monolayer at the water-air interface, the monolayer can be transferred to the solid surface during emersion (retraction) or immersion (dipping) through the water surface. Systematic study of the formation of these films was first performed by Langmuir and Blodgett. Formation of multilayers is also possible for amphiphilic molecules in which the head group is very hydrophilic and and the tail is an alkyl chain.[3]

Self-assembly provides a possibility to create films of organic molecules which are more strongly attached onto a surface than LB films are.[3] Self-assembly is a widely observed phenomenon in natural systems. For instance, some proteins have this property.[4,5] One of the most attractive characteristics of self-

assembled monolayers is the simplicity of their preparation. In the self-assembly process, organic molecules spontaneously chemisorb on the surfaces of solids. In the case of the liquid phase method, molecules are dissolved in an organic solvent and they spontaneously adsorb onto the surface of a substrate material (Figure 1.). A typical solvent is ethanol, but for instance isopropanol is sometimes used.

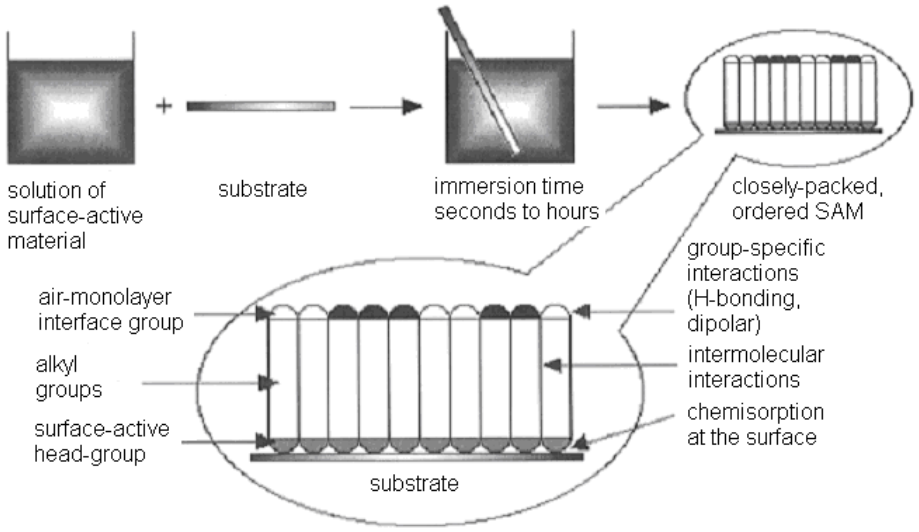


**Figure 1.** Self-assembled monolayers are formed by immersing a substrate into a solution of the surface-active material. The driving force for the spontaneous formation of the 2D assembly includes chemical bond formation of the molecules with the surface and intermolecular interactions.[6]

A pathway of the formation and ordering of alkanethiol monolayers on gold during the liquid phase adsorption has recently been drawn. The procedure starts from physisorbed thiols on a flat adsorption geometry. This is followed by dehydrogenation, leading to formation of a chemisorbed thiolate, and finally yielding densely packed films with the molecular axis tilted to an upright position. The procedure is presented in Figure 2. The growth of the lying-down phase follows the first-order Langmuir adsorption isotherm with a time-scale of minutes and is followed by a slower process that lasts hours or days and is best described by a second-order reaction.[7] The detailed growth behavior will undoubtedly depend upon a range of variables such as the growth environment, molecular rigidity and headgroup-substrate chemistry.[4,8]

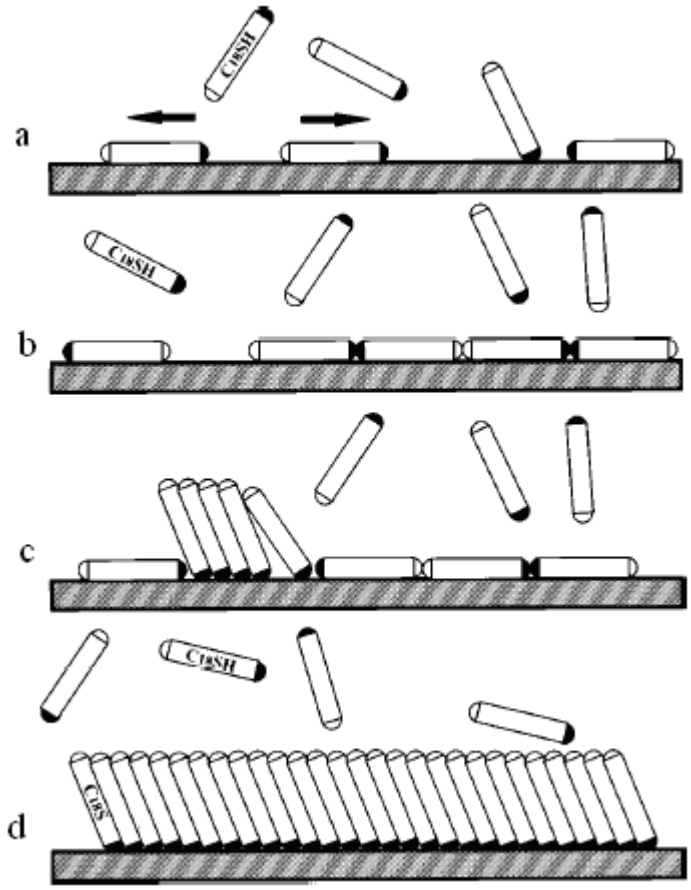


**Figure 2.** Schematic mechanistic diagram for the self-assembly of $CH_3(CH_2)_{17}SH$ on Au(111). a) Initial adsorption. b) Lying-down phase. c) Two-dimensional phase transition from a lying-down to a standing-up configuration. d) Formation of a complete SAM.[5]

In addition to liquid phase methods, other methods are also available for creating SAMs. One is to grow the film in an ultra high vacuum via vapor phase deposition. At low exposures, a striped phase will form on the surface. When the exposure is increased (> 300 L for Au(111) substrate) the striped phase disorders and the formation of the denser standing up phase begins. The adsorption process is driven by the evolution of a molecular coverage and can be described as a series of well-defined transitions of molecules on the surface as a function of coverage. The formation does not happen through a continuous variation in the local monolayer structure but through the coexistence of discrete phases.[4,9]

An other method of making SAMs is to use a stamping technique. In the stamping procedure an alkylthiol is absorbed into an elastomeric stamp made of poly(dimethylsiloxane), PDMS, and then transferred by bringing the stamp into contact with a clean metal surface. The use of elastomeric stamps to produce patterned SAMs was first introduced by Kumar et al.[10,11] In this way organic surfaces patterned with well-defined regions exhibiting different chemical and physical properties have been produced.

## 2.2. Structure of surface thiolates

The structural order of monolayers has been investigated as the packing and orientation of adsorbates affects the surface chemistry of monolayers. Forces acting at the molecular level in self-assembled monolayers play a major role in establishing the macroscopic properties of the monolayer. Organic molecules as building blocks provide a wide range of variety regarding both strength of interactions as well as directionality. Well-defined molecular structures can be created with tailored organic molecules.[12]

The structure formation is governed by the balance between intermolecular and molecule-substrate interactions.[12] The competing forces, which ultimately determine the SAM structure, are the interaction between the headgroup and the substrate and the interchain van der Waals dispersive forces. Although van der Waals interactions are comparatively weak, they can have a significant influence on molecular self-assembly of organic molecules possessing e.g. long alkane chains.[12] An ordered structure of chemisorbed molecules on a substrate surface is not governed only by intermolecular interactions but also by the strong chemisorption energy. Molecular self-assembly of chemisorbed species is possible when the mobility of the substrate atoms is high enough such that the chemisorbed molecule together with the bound substrate atom forms a new entity, which then can diffuse and act as a new building block. This is rather common effect upon molecular adsorption onto metal surfaces. Molecule deposition has been observed to cause both a local substrate restructuring as well as a large-scale surface refacetting.[12]

The formation of surface thiolates has been observed for different thiols on metal surfaces. Probably the most studied SAM system is 1-alkanethiols on gold. It has become a model system for developing self-assembled organic monolayers on metal substrates. The final SAM has a commensurate $\left(\sqrt{3}\times\sqrt{3}\right)R30^\circ$ structure on Au(111) (Figure 3.). The hexagonal packing of the

molecules with an additional c(4 × 2) symmetry is also observed. In addition to this superlattice structure, additional structures are found. Using different study methods a (6 × √3) final phase, slightly different c(4 × 2) phases, or a (3 × 4) superstructure and intermediate standing ($p \times \sqrt{3}$)phases have been observed.[13] On the basis of the $sp^3$ hybridization of the bonded sulfur atom upon chemical binding, the alkyl chain has an orientation of $\beta \approx 30^{\circ}$ from the normal to the Au(111) surface and a twist angle of $\gamma \approx 50^{\circ}$.[14] Definitions of β and γ are presented in Figure 4. Figure 5 presents the top and side views of hexylthiolate on Au. For the 1-dodecanethiol SAM the film thickness is about 1.5-1.8 nm.[15]

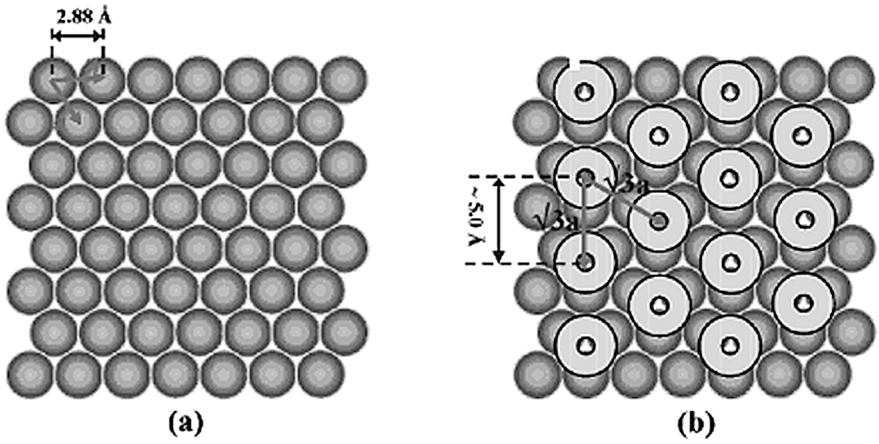


**Figure 3.** Structure and adsorption sites of Au(111) surface. (a) Top view of a clean (111) substrate. (b) Top view of an organic self-assembled monolayer with $\left(\sqrt{3} \times \sqrt{3}\right)R30^{\circ}$ surface structure. Each light-grey circle represents one organic molecule which chemically binds to a 3-fold adsorption site of the (111) substrate. The labeled structure parameters are for Au(111).[14]

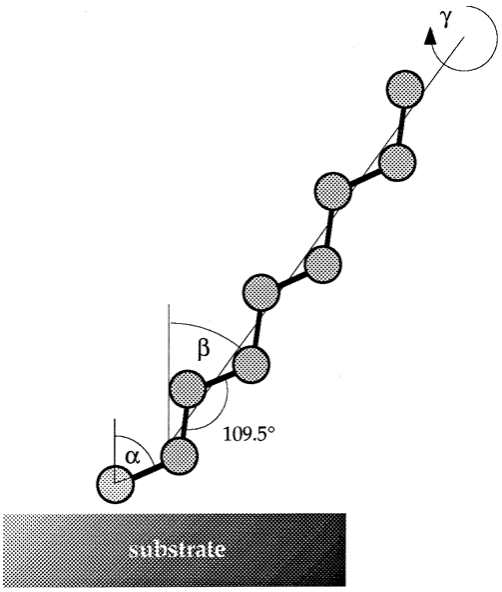


**Figure 4.** Schematic view of a single adsorbed molecule of 1-octanethiol, omitting H atoms for clarity. The chain axis is defined as being the line connecting the centers of the C-C-C bonds and is canted at the "tilt" angle β from the surface normal. The quantity γ is the "twist" angle of the C-C-C plane about the chain axis. The polar angle of the S-C bond is given by α.[16]

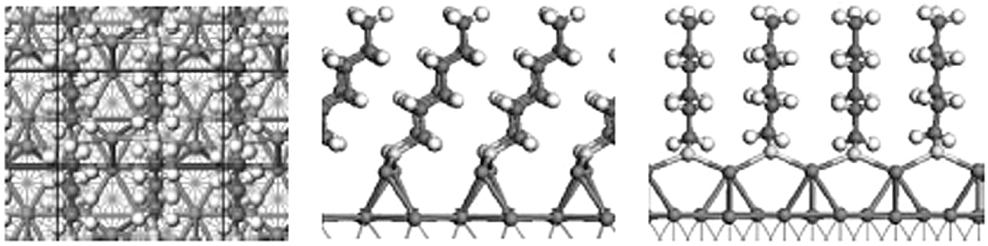

**Figure 5.** Top and side views of hexylthiolate in the $(RSAu)_x$ configuration.[17]

In this study, polycrystalline substrates have been the main interest. Polycrystalline metal substrates present a grain structure characterized by dense arrangements of intergrain boundaries, faceting, occlusions, twins, and other gross structural irregularities. Indeed, the substrates on which SAMs form are replete with many structural defects, and this reflects on the structure of the SAMs. Further, the cleanliness of the substrate, the methods for preparing the

substrate and other factors such as the purity of the solution of adsorbates are responsible for some defects in SAMs, but some are simply because SAMs are, in fact, dynamic systems with a complex phase behavior. Figure 6 illustrates some defects found in SAMs formed on polycrystalline substrates.[18]

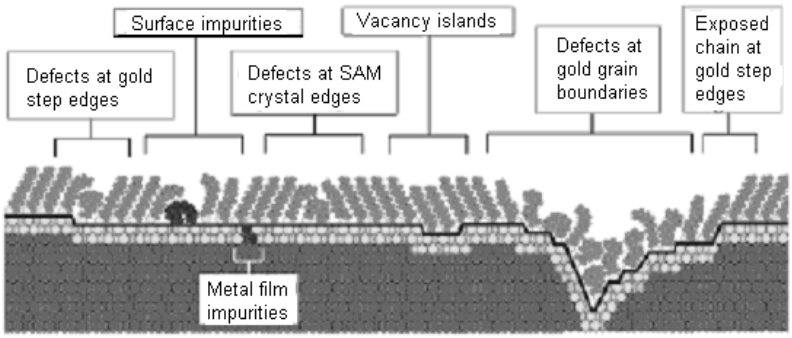


**Figure 6.** Schematic illustration of intrinsic and extrinsic defects found in SAMs formed on polycrystalline substrates. The dark line at the metal-sulfur interface is a visual guide for the reader and indicates the changing topography of the substrate itself.

Despite intense studies of SAMs, the precise nature of the sulfur/metal interaction and organization of molecules on surfaces remains unresolved in many cases. The accurate determination of the structure, composition, quality, and coverage of self-assembled monolayers (SAMs) is still under study.[19,20,21]

# 2.3. Methods to study thin organic layers

Accelerating the development of applications based on thin films will depend on the ability of researchers to more accurately characterize the physical and chemical properties of these systems. Self-assembled monolayers have been intensively investigated over the past decades and various techniques have been used. For example, XPS, AFM, STM, ToF-SIMS, FT-IR, Raman spectroscopy, contact angle measurements and ellipsometry have all been used to improve the knowledge of the chemistry, physical properties and molecular architecture of different SAMs.[20,22, 23,24,25,26]

# 2.4. Applications of self-assembled monolayers

Self-assembled organic monolayers are expected to show considerable technological potential. This method can be used to build up large structures from small building blocks. These structures have novel properties and functions because of their small size. Self-assembled monolayers have become one of the most important classes of surface coatings.

Self-assembled monolayers can be used for controlling the wetting properties of surfaces. The wetting and dewetting processes and the interaction of simple liquids, polymers, emulsions, and suspensions with surfaces are scientifically interesting and technologically important problems.[27,28,29,30]

SAMs are also used for lithographical applications and offer the most accessible and successful route to control the placement of molecules. Litographic patterning on length scales close to the size of molecules has been reached by adding, removing or replacing the molecules in the SAM. By controlling the location of molecules, the location of special functional groups on a surface can also be controlled and special chemical functionalities can be combined with the pattern.[31,32,33,34]

In the field of biology, self-assembled monolayers serve as a new tool to provide a model for biocompatible surfaces. SAMs can be used to immobilize peptides, proteins, and other biomolecules on the surfaces. Using SAMs of different structures, thickness and terminal groups as a sublayer, it is possible to clarify the influence of various surface factors on the adsorption and bioactivity of various biomolecules. With the combination of modern patterning techniques and novel synthetic strategies it is now possible to prepare complex, organic surfaces with well-defined structures and chemistry.[35,36,37,38]

Thiol self-assembled monolayers are also useful in the development of molecular electronics. SAMs on metal surfaces, particularly on Au(111), have served as models in the majority of recent studies of molecular electronics.[39,40,41,42,43]

SAMs can also protect metals against corrosion.[44,45,46] In many studies, alkanethiol monolayers have been found to produce effective barriers to the penetration of corrosive chemicals on the substrate metal surface and to limit the oxidation of the substrate. For example, silver surfaces with octadecanethiolate monolayers could be kept in ambient conditions without

tarnishing for many months, and copper surfaces coated with the same monolayer sustain nitric acid.[6]

# 3. Aim of the study

The details regarding the nature of the metal-sulfur bond and a spatial arrangement of the sulfur groups on the underlaying gold lattice are still controversial. There is even less knowledge concerning the reactions for forming SAMs from organosulfur compounds on other metals, such as copper, silver and platinum. All these systems have been studied in some detail, but each metal has a different structural surface chemistry and a different reactivity toward organosulfur compounds. These variations of substrates and molecules impact the assembly process in significant ways and lead to a variety of structural motifs that are distinct for each other.[15] The nature of the substrate-adsorbate interaction plays a major part in deciding the ultimate structure of the SAM.

The most important aims of the current work were:

• To increase an understanding of the differences and similarities between the SAMs on different substrate materials. Gold, silver, copper and platinum are all substrate materials that have been used to form SAMs of technological interest.

• To study the dependence of the monolayer formation on the cleanliness of the substrate material. For industrial applications the possibility for the air exposure during the manufacturing process is a valuable quality.

• To demonstrate the capabilities of XPS in the SAM research area but also the challenge related to radiation induced damages to the SAMs originating from the electrons excited in the photoemission process causing chemical dissociation processes in the adsorbed molecules as well as breaking of the adsorbate-substrate bonds.

# 4. Experimental methods

## 4.1. Photoelectron spectroscopy

Core-level photoelectron spectroscopy is a method for analyzing elemental composition and chemical states of surfaces.[47,48] Because of its applicability for chemical analysis, the method is also called ESCA (Electron Spectroscopy for Chemical Analysis). The sample is positioned in a vacuum chamber and irradiated with a photon beam. Two basic interaction processes that dominate on the interaction of X-rays with solid matter are the photoelectric effect and X-ray scattering. In photoelectron spectroscopy, the photoelectric effect is of interest. The kinetic energy of the emitted photoelectrons is analyzed and their binding energies can be calculated. The energies involved can be given by the Einstein relation[47]

$$E_K = h\nu - (E_B + \phi_{SPECTROMETER}) \quad (1)$$

where $E_K$ = kinetic energy of the ejected photoelectron
$h\nu$ = characteristic energy of incident photon
$E_B$ = binding energy of core-level electron
$\phi$ = work function of the spectrometer.

This equation can be described graphically as shown in Figure 7.

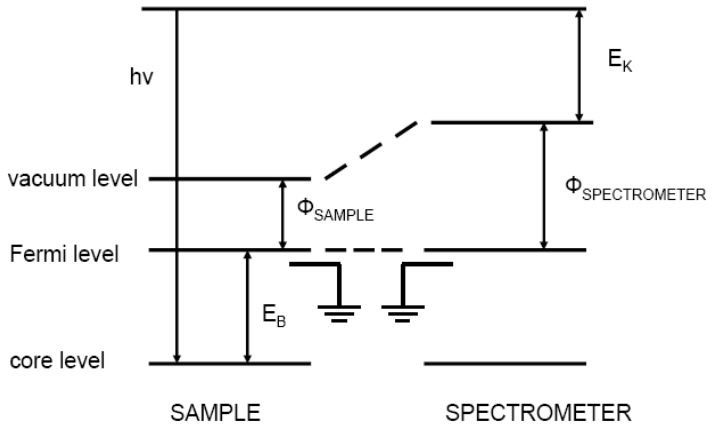


**Figure 7.** The energy level diagram for photoelectron spectroscopy.

The definition of the binding energy $E_B$ of the photoemitted electron is the following: A photoemission process produces a final state (*f*) that is lacking one electron with respect to the initial state (*i*). $E_B$ is the difference of the total energy of the system (atom with N electrons) before excitation $E_i$ and the total energy of the system (atom with N-1 electrons (ion) and free photoelectron) after excitation $E_f$

$$E_B = E_f - E_i \tag{2}$$

The measured value of $E_B$ is not a value of orbital energy. After ejection of one electron the system readjusts its remaining charges to minimize its energy. This is called a relaxation process and it affects $E_f$. In a solid matter, the relaxation energy consists of two basic contributions: one results from the relaxation of the orbitals of the same atom (intra-atomic relaxation). The other one is due to the charge flow from the crystal onto the ion that carries the hole (extra-atomic relaxation).

## 4.1.1. Structure of photoelectron spectra

The photoelectron spectrum is a plot of the number of detected photoelectrons per energy interval versus their binding energy. The spectrum is a direct reflection of the electronic structure of the electron emitting atom in solids (Figure 8.). The peaks in the spectrum can be grouped into three basic types: peaks due to photoemission from core levels and valence levels and peaks due to X-ray excited Auger emission. In addition to these peaks, satellites may also appear in the spectrum due to plasmon structures, shake-up, shake-off and other energy loss processes. However, the most intense peaks are typically due to photoemission from core levels.

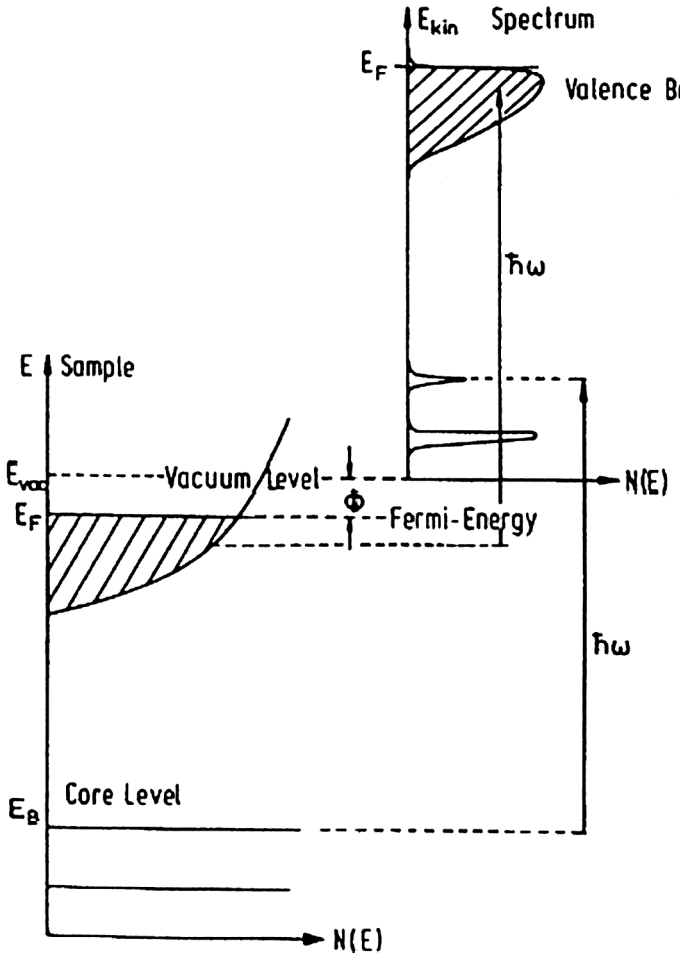


**Figure 8.** Relation between the energy levels in a solid and the electron energy distribution produced by photons of energy ħω.[48]

The spectrum from a sample composed of several elements is a sum of the components of the individual constituents. This means the total spectrum measured from a long energy range gives an elemental composition of the sample surface. For example, a range from 0 to 1100 eV can be chosen, since all elements produce peaks between those energy values. More detailed analysis of the chemical states of the elements can be made with a detailed analysis of individual peaks. In this research, the core level photoelectrons have been the main interest. The binding energy values and shapes of the core level photoemission lines have been studied in order to get information about the sample surface.

The core level binding energies are sensitive to local electronic structure and therefore depend on the chemical surroundings of the photoemitting atoms. The change in binding energy of a core electron of an element due to a change in the chemical environment of that element is a chemical shift.[49,50] The existence of these shifts, their direction and magnitude, makes the method ideal for detailed chemical analysis.[51] Non-equivalence of atoms can arise in several ways: for example, a difference in the formal oxidation state, in the molecular environment and in the lattice. Whatever the case, shifts in core electron binding energies vary with the chemical environment of the perturbed atom mainly through a quasi-linear dependence upon the net charge transferred from the bonded atoms or chemical groups, or the surrounding molecules.[52] The mechanisms behind chemical shifts are very involved and not straightforward to predict.

The peak width, defined as the full width at half-maximum (FWHM), is a convolution of several contributions: the natural or inherent width of the core-level, the width of the photon source and the analyzer resolution. Peak shapes are typically determined by a Gaussian broadening, mostly due to incoming radiation and the measurement process in the spectrometer and a Lorenzian contribution due to the limited lifetime of the core hole state. Gaussian contributions may also be related to phonon processes. Chemical, structural, and electronic inhomogeneities in the surroundings of the emitting atoms also often contribute to the Gaussian broadening.[47,53]

Due to a more complex photo excitation process, most metal signals exhibit inherently asymmetric peak shapes. Electronic excitations in metallic systems can cause the creation of electron-hole pairs at the Fermi-level introducing an asymmetric tail to the higher binding energy side of the core level peak. This is a well known phenomenon when the sample material is platinum, for instance.

## 4.1.2. Fitting procedure

The fitting procedure is adequately described, for example, in the article describing peak shape analysis of core level photoemission spectra using the Unifit for Windows program.[53] The procedure is always started with a background subtraction. The shape of the spectrum background may be affected by inelastic energy loss processes, secondary electrons and nearby peaks. After the background subtraction, the core level spectrum is analyzed. The procedure is focused on the lines' position determination and peak shape analysis. The experimental data is compared to theoretical model curves. A

description of the core level line shape may be modelled mathematically by a convolution of independent Gaussian and Lorentzian (or Doniach-Šunjić type) functions. This Voigt profile is defined as follows:[53]

$$f(E)=f(L*G)=\int_{-\infty}^{\infty} L(E')G(E-E')dE' \tag{3}$$

Both the height-normalised Lorentzian function *L(E)*:

$$L(E)=\left\{1+\left[\frac{(E-E_0)}{\beta}\right]^2\right\}^{-1} \tag{4}$$

and the Gaussian function *G(E)*:

$$G(E)=\exp\left\{-\ln 2\frac{(E-E_0)^2}{\beta^2}\right\} \tag{5}$$

are completely determined by the peak parameters $\beta$ and $E_0$, representing *FWHM/2* and the peak position, respectively.

Asymmetric peak shapes may be taken into account by substituting the Lorentzian broadening by the Doniach-Šunjić (DS) peak shape.[54] It may describe the low-energy tail of the peak caused by the many body effects and it is determined by the value of the asymmetry parameter $\alpha$. *DS(E)* is given here as:[53]

$$DS(E)=\beta\frac{\cos\left\{\pi\frac{\alpha}{2}+(1-\alpha)\arctan\left[\frac{(E-E_0)}{\beta}\right]\right\}}{\left[(E-E_0)^2+\beta^2\right]^{\frac{1-\alpha}{2}}} \tag{6}$$

Notice that the Doniach-Šunjić peak shape converges into a Lorentzian function at the limit of $\alpha \rightarrow 0$. The line shapes described above are in common use although other profiles can be applied for certain cases.

## 4.1.3. Surface sensitivity of photoelectron spectroscopy

In conventional X-ray photoelectron spectroscopy (XPS) equipment either an aluminium or magnesium anode is used to produce the X-ray beam by bombarding it with electrons. The energy of the Al Kα line is 1486.6 eV and the energy of the Mg Kα line is 1253.6 eV. The X-ray beam of this energy penetrates into the sample down to a depth of 1-10 μm.

Photoelectrons have a relatively large probability of inelastic scattering in the near-surface region.[55] Thus, the surface sensitivity of XPS is roughly based on the inelastic mean free path $\lambda_{IMFP}$ of electrons. The formalism is related to the assumption that photoelectrons move inside the solid along a straight line from the point of emission to the surface.[56] The surface sensitivity of photoelectron spectroscopy can be presented in a universal curve (Figure 9), which shows the dependence of IMFP of electrons on the emitted electron kinetic energy for elements.[57] It describes the idea of the surface sensitivity of XPS being quite independent of elements and depending only on electron energy.[58] However, the material dependence of the IMFP can not be totally ignored.[55] In reality, the electrons may be elastically scattered by atoms within the surface region. This phenomenon may partially randomize the direction of the electron motion, and consequently may affect the probability for the electron to leave the solid without an energy loss. Correction factors that account for elastic scattering effects in XPS have been determined.[56] One has to particularly take into account the fact that the absolute values of the IMFP of electrons in materials such as inorganic solids and polymers differ quite significantly from those in metals.

For determination of the average depth of analysis, mean escape depth, MED, should be used.[58] If the effects of elastic electron scattering are neglected, the mean escape depth can be defined as a distance normal to the surface at which the probability of an electron escaping without any significant energy loss due to inelastic scattering processes drops to $e^{-1}$ of its original value.[55,59] In this case, the relation of mean escape depth (*MED*) of the detected electrons to the inelastic mean free path of electrons ($\lambda_{IMFP}$) in XPS is given simply by

$$MED = \lambda_{IMFP} \cos\alpha \tag{7}$$

where $\alpha$ is the electron emission angle with respect to the surface normal.[60]

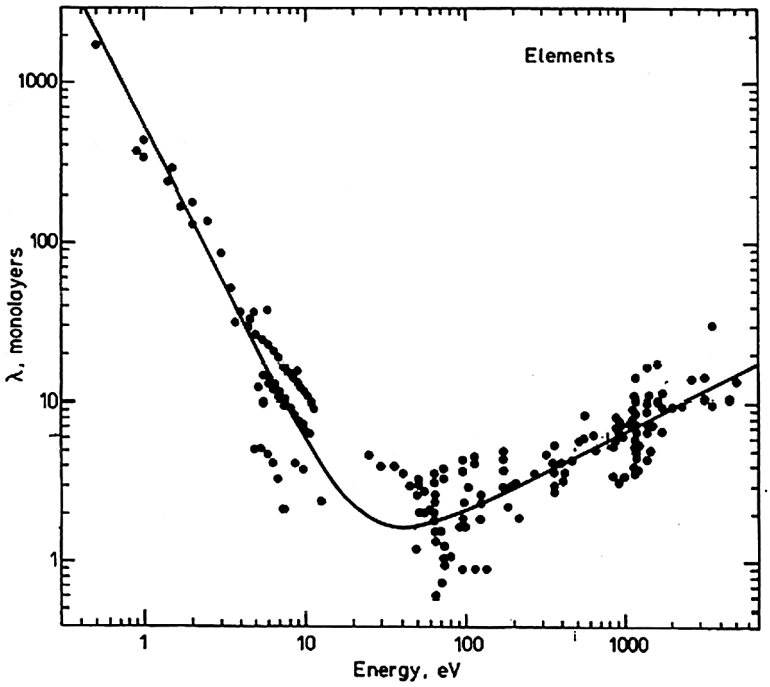


**Figure 9.** Universal curve. The dependence of $\lambda$ (in monolayers) on electron kinetic energy (eV). In the presented compilation of IMFP measurements the material through which the electron passes is elements.[57]

In order to achieve maximum surface sensitivity the photon energy should be adjustable so that the kinetic energy of the electrons of interest can be placed in the 20-100 eV range. By using a synchrotron to produce excitation energy one has a continuously tunable source of photons from a wide energy range including infrared, visible, ultraviolet and X-ray regions.[61] The basic idea of a synchrotron radiation is based on the fact that charged particle emits radiation when accelerated.[62] If electrons or positrons moving at relativistic velocities are deflected along a curved trajectory by a magnetic field, they radiate in a narrow forward cone and synchrotron radiation is produced.

Some of the experiments performed in this thesis were carried out at the MAX-lab synchrotron facility in Lund, Sweden. A schematic view of MAX-lab is presented in Figure 10. At the MAX-lab a linear accelerator (LINAC) is used to produce an energetic electron beam. Accelerators employ electric and magnetic fields to accelerate, focus and steer the charged particles. Particles are then injected into a storage ring. In the storage ring, particles are stored with a constant energy, moving near the speed of light. The major components of the

storage ring are a radiofrequency cavity which restores the energy that circulating particles lose in the emission of synchrotron radiation, focusing sets of magnetic quadrupoles which keep the particles in bunches, bending magnets to keep particles in a closed trajectory and insertion devices (undulators and wigglers). The radiation is taken out from a port in the ring and guided through a beamline (BL). The beamline I411 starts with an undulator. The undulator consists of a periodic structure of dipole magnets. Electrons traversing the periodic magnet structure are forced to undergo oscillations and radiate. The radiation produced in an undulator is very intense and concentrated in narrow energy bands (Figure 11). By varying the gap of the undulator magnet lattice it is possible to tune the energy of emitted photons.

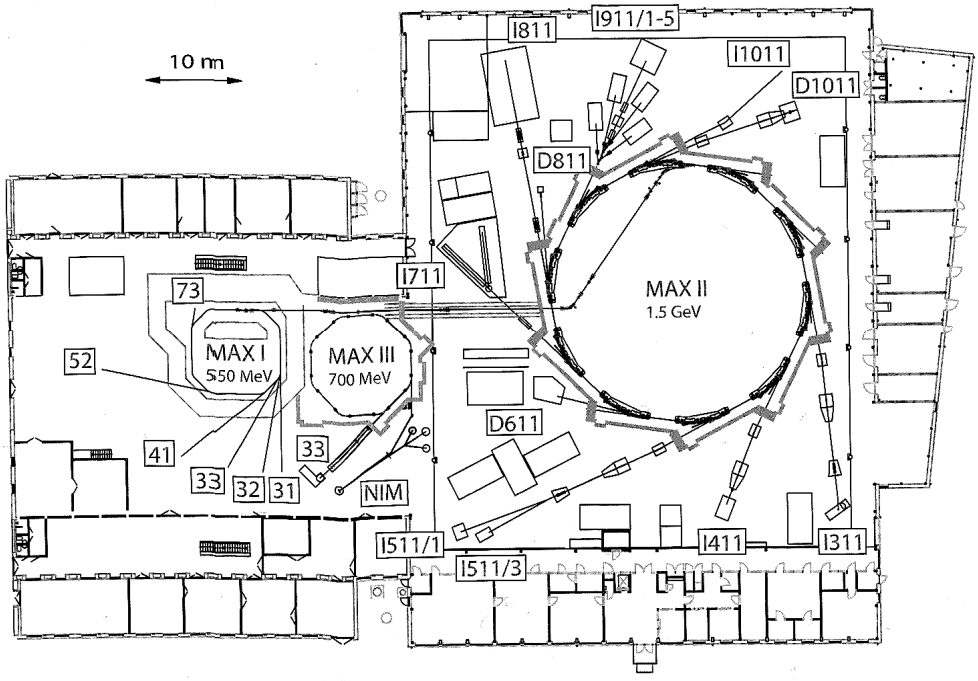


**Figure 10.** A schematic view of MAX-lab synchrotron facility in Lund, Sweden.[63] In these studies beamline I411 of MAX II was utilized.

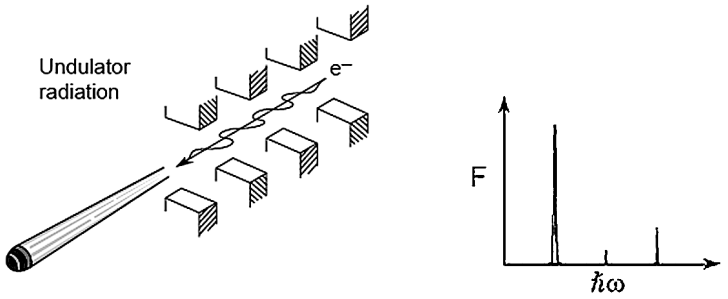


**Figure 11.** The principle of an undulator on the left and the energy spectrum obtained from undulator on the right.[64] Electrons moving in the periodic magnet structure undergo oscillations and radiate. The radiation produced in an undulator is very intense and concentrated in narrow energy bands.

## 4.1.4. Quantitative analysis with XPS

With XPS quantitative analysis of the elemental composition of a sample can be obtained. The peak areas, together with spectrometer sensitivity factors, can be used to determine the atomic concentration of the sample. The easiest point to start is the formulation of simple linear expression where the intensity of the signal $I_A$, from element $A$ in a solid is simply proportional to the molar fractional content, $X_A$, in the analysis depth. Thus:

$$X_A = \frac{I_A}{I_A^\infty} \tag{7}$$

where $I_A^\infty$ is the intensity from pure $A$. Since, in general, $I_A^\infty$ is not known but the ratio $\frac{I_A^\infty}{I_B^\infty}$ can be found, the more useful form of the above equation becomes

$$X_A = \frac{I_A / I_A^\infty}{\sum_{i=A,B} I_i / I_i^\infty} \tag{8}$$

where $B$ is another constituent of the solid, and the sum is over all of the constituents of the solid.[47,65]

One has to be aware of the facts which need to be taken into account for a more precise quantitative analysis by XPS. First of all, the technique cannot be applied rigorously to heterogeneous samples. Moreover, the escape probability for the emitted photoelectron depends strongly on the elastic and inelastic scattering of photoelectrons.[56,66,67]

## 4.2. Time-of-flight secondary ion mass spectrometry

The ToF-SIMS method is based on the sputtering of the sample. It uses a pulsed primary ion beam to remove and ionize species from the sample surface. When a high energy (normally between 1 and 15 keV) beam of ions bombards the surface, the particle energy is transferred to the atoms of the solid by a billiard-ball-type collision process. Typically, liquid metal ions such as $Ga^+$, $Cs^+$ or $O^-$, are used to bombard the sample surface. The bombarding primary ion beam produces monatomic and polyatomic particles of the sample material and resputtered primary ions, along with electrons and photons. The secondary particles carry negative, positive, and neutral charges and they have kinetic energies that range from zero to several hundred eV. The vast majority of the emitted species are neutral but it is the secondary ions which are detected and analyzed. The yield of secondary ions is strongly influenced by the electronic state of the material being analyzed. The basic SIMS equation is

$$I^m{}_s = I_p y_m \alpha^+ \theta_m \eta \tag{9}$$

where $I^m{}_s$ is the secondary ion current of species $m$, $I_p$ is the primary particle flux, $y_m$ is the sputter yield, $\alpha^+$ is the ionization probablity to positive ions, $\theta_m$ is fractional concentration of $m$ in the surface layer and $\eta$ is the transmission of the analysis system.[68]

The resulting secondary ions are accelerated into a mass spectrometer, where they are mass analyzed by measuring their time of flight from the surface to the detector. According to the equation of kinetic energy, heavier masses travel more slowly through the flight tube and so the measured flight time, $t$, of ions of the mass-to-charge ratio, $m/z$, accelerated by a potential $V$ down a flight path of length $L$ provides a simple means of mass analysis according to following equation[68]

$$t = L\sqrt{\frac{m}{2zV}} \tag{10}$$

A mass spectrum of the surface can be obtained and it enables a detailed chemical analysis to be performed. All elements and their isotopes can be detected. When the sputtering rate is extremely slow, the entire analysis can be performed while consuming less than a tenth of an atomic monolayer. This slow sputtering mode is called static SIMS in contrast to dynamic SIMS used for depth profiling. A shematic representation of ToF-SIMS instrumentation is presented in Figure 12. A more extensive introduction can be found in refs. [68,69,70]

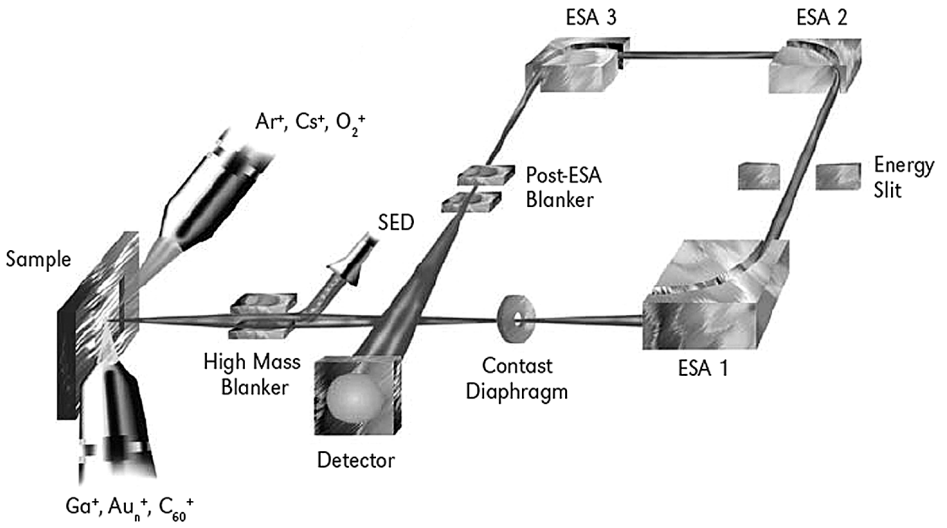


**Figure 12.** A shematic representation of TRIFT ToF-SIMS instrumentation.[71] Submicron pulsed beam of $Ga^+$ primary ions collide with the sample surface. Characteristic secondary ions are desorbed from the surface. Secondary ions are analyzed and detected using TOF mass analyzer.

ToF-SIMS analysis yields elemental and molecular data. It can be used to characterize both organic or inorganic and insulating or conductive samples. However, analyzing insulators is possible only if the surface charging is eliminated, for example, by bombardment with low energy electrons. SIMS is widely used for analysis of thin films. Figure 13. presents some oligomers that are emitted by negative ion emission from an octanethiol SAM on gold. A chemical map of a surface can also be generated. An image is created by rastering a finely focused beam across the sample surface. The entire mass spectrum is acquired from every pixel in the image. A problem with the method is that secondary ion yields vary depending on the surface material which was presented in equation 9. This makes quantification difficult, because there is no simple relationship between the intensity of the mass peak and the

concentration of a particular element on the surface. The surface roughness also influences the spectra and peak intensities.

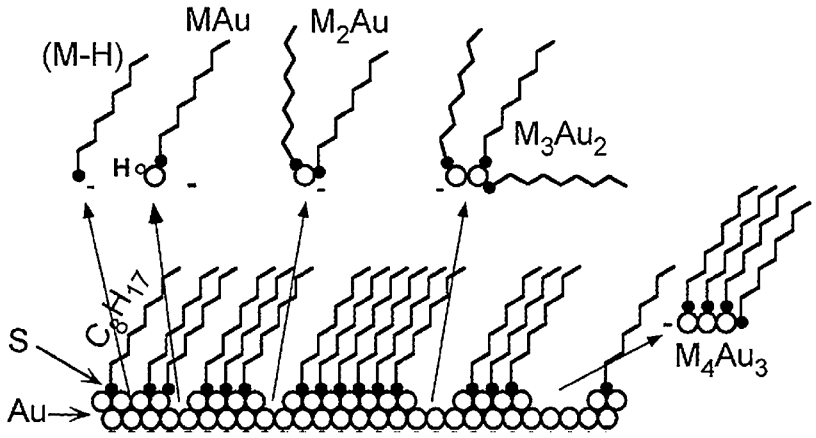


**Figure 13.** Schematic representation of monomers, dimer, trimer and tetramer negative ion emission from an octanethiol SAM on gold.[72]

# 5. Experiments

## 5.1. Materials

Polycrystalline metal (gold, platinum, silver, or copper (Goodfellow, Outokumpu Copper)) samples of about size 5×5×2 mm were used as substrates. In some measurements the Pt(111) single crystal (Mateck) disk was used.

Dodecanethiol, $CH_3(CH_2)_{11}SH$, was used for chemical treatment of the sample. Thiol was used as purchased from Aldrich (99 %). In one series of studies Sodium S-Dodecylthiosulfate, $CH_3(CH_2)_{11}SSO_3Na$, was also used, and prepared according to the method described by Peak and Watkins.[73] Briefly, 24.9 g (0.1 mol) of 1-bromododecane was dissolved in 50 mL of ethanol and 25.0 g (0.1 mol) of $Na_2S_2O_3 \cdot 5H_2O$ in ca. 500 mL of water was added. The mixture was refluxed for 3 h and the white precipitate (a monohydrate) was filtered and recrystallized from ethanol.

The treatment solution was made into an absolute ethanol (AA). An Elgastat UHQ II water purification unit was used to get pure water and the glassware used was washed with piranha-solution. Piranha-solution consists 70 % $H_2SO_4$ and 30 % $H_2O_2$ (30 % $H_2O_2$ in water). This solution must be handled with care because it is extremely oxidizing and reacts violently with organics, and it should only be stored in loosely tightened containers to avoid pressure buildup.

## 5.2. Sample preparation

In the studies presented in paper III, special attention was paid to the preparation of oxygen-free metal surfaces. In the case of gold, the polycrystalline disk electrode was first polished with 0.03 μm alumina, sonicated in Millipore water and then cycled in 0.5 M $H_2SO_4$ until the voltammogram of pure gold was obtained. In the case of platinum, the electrodes were cleaned in oxygen plasma, followed by a treatment in hydrogen plasma. These procedures have been shown to produce clean gold and platinum surfaces.

In the other measurements (papers I, II, IV and V), the sample treatment was kept as simple as possible. A typical sample treatment method was as follows: polycrystalline samples were wet polished with 4000 MESH SiC grinding paper (Struers), washed with clean water and immersed into the treatment solution. This easier method of preparation was chosen to be the main cleaning method, since no differences between the S 2p line of samples prepared by different methods were obtained. The electrodes were placed in the treatment solution directly after the cleaning procedures.

The Pt(111) sample was cleaned by repetitive $Ar^+$ bombardment and heating in an ultra high vacuum (UHV) until the characteristic LEED pattern was obtained and XPS indicated a clean surface. Again, the electrodes were placed in the treatment solution directly after the cleaning procedures.

Layers were formed by spontaneous adsorption onto the metal surfaces. A freshly prepared 1 mM solution of 1-dodecanethiol in ethanol was used. The solution was bubbled with nitrogen or argon gas to remove oxygen. The solution chamber was closed after 15 minutes of immersion of the sample and left in the dark. Samples were kept in the solution 12-24 hours and, after monolayer formation, were rinsed thoroughly with ethanol and pure water.

# 5.3. Surface analysis

## 5.3.1. X-ray photoelectron spectroscopy

XPS measurements were performed at the Laboratory of Materials Science with a Perkin-Elmer PHI 5400 spectrometer. All XPS data was recorded using analyzer pass energy of 35.75 eV and a step width of 0.1 eV for detailed scan spectra and 89.45 eV and 0.5 eV for wide scan survey spectra. The binding energy scale of the spectrometer was calibrated by using the standard Au $4f_{7/2}$ reference line (BE = 84.0 eV). The electron take-off angle was 45° if no other value is mentioned. Monochromatized Al Kα radiation (hν = 1486.6 eV, 14.5 kV, 300 W) was normally used. For special purposes (such as increasing the volume of the beam) unmonochromatized Mg Kα radiation (hν = 1253.6 eV, 14.5 kV, 200 W) was used. Measurements were done at room temperature and the base pressure in the analyzer chamber was ca. $2\times10^{-9}$ torr. during spectrum acquisition. The spot diameter of the analyzed area was about 2 mm.

## 5.3.2. Synchrotron based high resolution X-ray photoelectron spectroscopy

The synchrotron based high resolution core level X-ray photoelectron spectroscopy studies presented in this thesis were carried out at MAX-lab (National Electron Accelerator Laboratory for Synchrotron Radiation Research, Nuclear Physics and Accelerator Physics) in Lund, Sweden. The beamline I411 at MAX II storage ring was used. This beamline has a high brilliance undulator photon source and it covers the photon energy range from 50 eV to about 1500 eV. The photons are monochromatized by a Zeiss SX-700 plane grating monochromator. The final part on the beamline is the end station equipped with an angle resolved Scienta SES-200 analyzer. With this equipment the spectral resolution is always less than 100 meV, typical value for the measurements of S 2p spectra was 40 meV.[74,75]

## 5.3.3. Peak fitting

The peak shapes of the core level photoelectron spectra were analyzed with the Unifit program or sometimes with an Origin Peak Fitting Module. The Unifit program is presented in the article by R. Hesse.[53] In this study, a Shirley or linear type background correction and a Gaussian-Lorenzian peak shape (Voigt function) or asymmetric peak shape were used. The binding energy of the most intense line from the metal substrate was normally used as an internal standard to correct the possible binding energy shift, for synchrotron based measurements also the energy of the Fermi level of metal was defined in each case. Photoelectron spectra of S 2p, C 1s, Au $4f_{7/2}$, Ag $3d_{5/2}$, Pt $4f_{7/2}$ or Cu $2p_{3/2}$ were always recorded during a single experiment. The O 1s line was also always measured. The atomic concentrations were obtained from a long energy range XPS spectra by using the spectral intensities divided by experimental sensitivity factors provided by the spectrometer manufacturer.

## 5.3.4. Time-of-flight secondary ion mass spectrometry

Time-of-flight secondary ion mass spectrometry (ToF-SIMS) measurements were performed at the Top Analytica Ltd. with a Physical Electronics TRIFT II

(Physical Electronics Inc., Eden Prairie, USA) device. The instrument was equipped with a liquid metal $^{69}Ga^{+}$ primary ion gun and a high mass resolution time-of-flight mass analyzer.

Thin organic layers are very sensitive to ion beam damage. The situation was taken into account by performing all the ToF-SIMS measurements under static conditions. Positive and negative ion mass spectra were detected from an area of 200×200 $\mu m^2$. The WinCadence program was used for the analysis of the measured mass spectra. The peak assignments were made on the basis of the exact mass value and the isotopic distribution of elements.

## 5.3.5. Electrochemistry

The impedance spectroscopy measurements of the SAMs formed from 1-dodecylmercaptan or S-dodecylthiosulfate were carried out with a VoltaLab PGZ301 potentiostat/galvanostat electrochemical impedance meter (Radiometer, Copenhagen) and the data analyzed by Boukamp's fitting software.[76] A conventional one-compartment three-electrode cell was used. The reference electrode was a saturated calomel electrode. A Pt wire served as a counter electrode. The results were calculated per geometrical area of the electrode. SAMs for impedance measurements were prepared by immersing evaporated Au thin film electrodes in deaerated 1 mM solutions of $CH_3(CH_2)_{11}SH$ or $CH_3(CH_2)_{11}SSO_3Na$ in ethanol for 24 h under an argon atmosphere. The emphasis was put on the comparison of SAMs prepared from thiols and thiosulfates under identical conditions. The impedance spectra were measured in aqueous solutions that were 2.5 mM with respect to $K_4[Fe(CN)_6]$ and $K_3[Fe(CN)_6]$ and 1.0 M with respect to KCl. All solutions used were deaerated with argon and all the measurements were carried out at room temperature.

## 5.3.6. Contact angle measurements

A CAM 200 optical contact angle meter (KSV Instruments, Ltd., Espoo, Finland) equipped with a video camera was used to measure the static aqueous contact angles. The measurements were performed at five different locations with at least two different samples. All measurements were carried out on thoroughly rinsed samples (ethanol and 18 MΩ water) immediately after removing the substrates from the modification solutions.

# 6. Results

In this study, XPS was the main method used to analyze engineered thin organic films. The presence of a layer of thiol molecules attached to the surface was indicated by a large increase in the carbon and sulfur peak intensities and a decrease in the metal peak intensities of the XPS survey spectra. The appearance of carbon and sulfur peaks was due to the existence of the layer. The modification of SAMs by radiation was considered. Special effort was paid to the interpretation of SAM-platinum system. The influence of oxygen on the formation of SAM was also studied. The results were compared with ToF-SIMS measurements.

## 6.1. Modification of SAMs by radiation

Some damage to SAMs resulted from the XPS measurements. The damage produced in SAMs by X-ray photons can be essentially related to the low-energy electrons arising through the inelastic scattering of the primary electrons created within the photoemission process.[77,78] In alkanethiolate SAMs, both the alkyl chains and the S-metal interface area are affected through the electron-induced dissociation of C-H, C-C, C-S and substrate-thiolate bonds. The defects and damages induced in alkanethiol monolayers have to be considered carefully when using XPS to study these systems.

### 6.1.1. Damage on Au and on Pt (Paper I)

When we studied the X-ray induced irradiation damage in the $CH_3(CH_2)_{11}SH$ monolayers on gold and platinum surfaces, we found that during the modification of the surface the thiol/platinum system behaves differently than the thiol/gold system. This behaviour is presented in Figure 14. On platinum, there are two chemically different sulfur species in pristine monolayers and their ratio remains unchanged as a function of measurement time. On gold, there is only one doublet at the beginning of the X-ray exposition, but another doublet grows to the higher binding energy side of the thiolate doublet as a function of measurement time. The existence of two components in the S 2p spectrum of the pristine $Pt/C_{12}SH$ monolayer is noteworthy. The S $2p_{3/2}$ binding energies were examined.

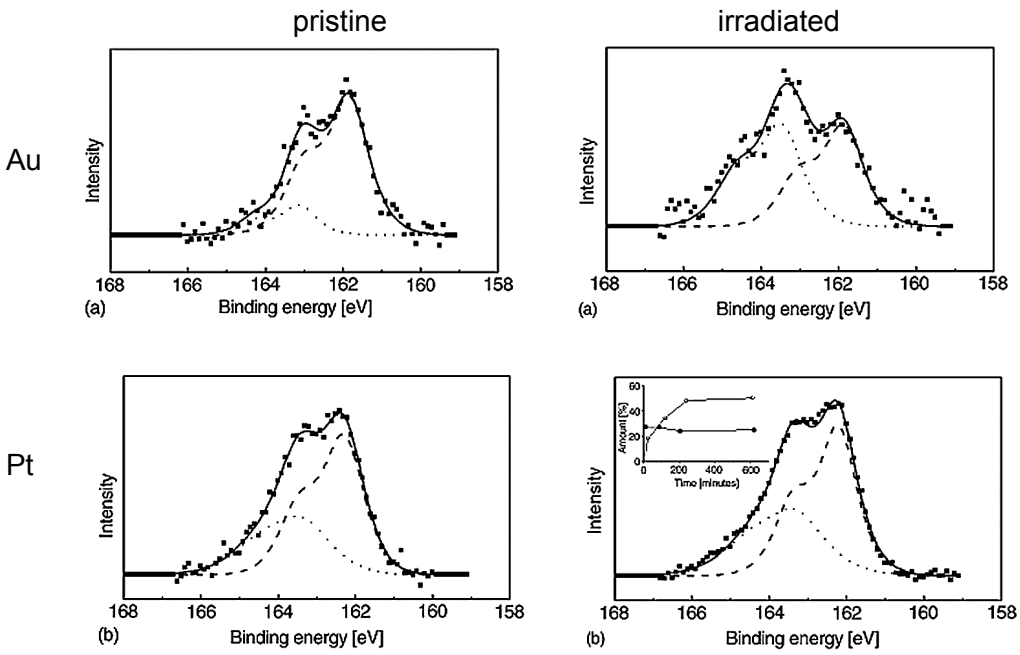


**Figure 14.** On the left side of the figure XPS spectra of S 2p emission from pristine thiol SAMs on gold (total irradiation time 24 min) and on platinum (total irradiation time 90 min) substrates. On the right side XPS spectra of S 2p emission from irradiated thiol SAMs on gold (total irradiation time 609 min) and on platinum (total irradiation time 621 min) substrates. Inset shows the percentage of the irradiation induced sulfur as a function of irradiation time. (○) on Au, (●) on Pt. Lines are shown only as a guide to the eye. The figure is adapted from Paper I.

If the substrate material was gold, only one doublet at the BE 161.9 eV was observed at the beginning of the measurement session and another doublet grew in the spectrum at the BE 163.3 ± 0.1 eV. The lower BE doublet was assigned as gold thiolate and the higher BE doublet as new irradiation induced sulfur species. New sulfur species have been assigned earlier as disulfide[24] or as sulfur incorporated into the alkyl matrix, i.e. dialkyl sulfides formed within the layer.[23] The S–C bond cleavege, according to the reaction RS – Au(s) + H → RH + S – Au(s) has also been reported.[79,80] The S $2p_{3/2}$ binding energy for atomic sulfur formed by the C–S cleavage has been reported to be around 161 eV,[81] whereas no components were observed in our spectra.

The spectra of the Pt/$C_{12}$SH SAMs were not affeced by the irradiation. In this monolayer two sulfur species with binding energies 162.3 ± 0.1 eV and 163.3 ± 0.2 eV were found. The relative inertness of the thiol SAMs on platinum was attributed to the stronger metal-sulfur bonds in this case. Again, the smaller BE can be connected to thiolate. The other component on the S 2p spectra from platinum substrate has the same binding energy as the irradiation induced sulfur species in the corresponding monolayer on gold. We have suggested possible explanations for this latter component on platinum. First, chemisorbed sulfur on Pt(111) has been shown to desorb thermally, partly as dimers.[82] Therefore, the higher binding energy could correspond to a dimerized thiolate species. This suggestion has been presented elsewhere and was based on earlier results obtained with sulfur[83] and mercaptopyridine[84,85] layers on platinum. Secondly, there might be different binding sites (bridge and hollow sites) for the thiolate head group on the Pt surface as has been suggested for methanethiol on some other transition metal surfaces.[86,87,88] This possibility does not exclude the existence of dimerized sulfur species but may, in fact, favour dimerization. However, platinum is a very active metal and a catalytic decomposition of the thiol molecules upon self-assembly may produce reactive sulfur and carbon species, which can form dialkyl sulfides on the surface. Dialkyl sulfides have been recently identified as the new sulfur species produced by X-ray irradiation inside the monolayers.[23] The same binding energy of the second sulfur species in pristine SAMs on Pt and irradiated SAMs on Au supports this conclusion.

## 6.1.2. Damage on Ag and on Cu (Paper II)

X-ray induced irradiation damage has been studied in the $CH_3(CH_2)_{11}SH$ monolayers on copper and silver surfaces. Surfaces have been characterized with X-ray photoelectron spectroscopy (XPS) using both synchrotron radiation and conventional Mg Kα excitation. Irradiation induced changes in thiolate SAMs on Ag (Figure 15) and Cu (Figure 16) were observed. The identification of the sulfur species has been achieved.

In the Ag/$C_{12}$SH system, the following binding energies of 160.9, 161.9, 163.4 for sulfur $2p_{3/2}$ are typically observed. The lowest binding energy peak (160.9 eV) is in a region characteristic of metal sulfides and it can be assigned to chemisorbed sulfur. The S $2p_{3/2}$ BE 161.9 eV can be attributed to surface thiolate. The relative intensity of the doublet with the S $2p_{3/2}$ BE at 163.4 eV increases significantly as a function of measurement time. This component is referred to as irradiation induced.[79]

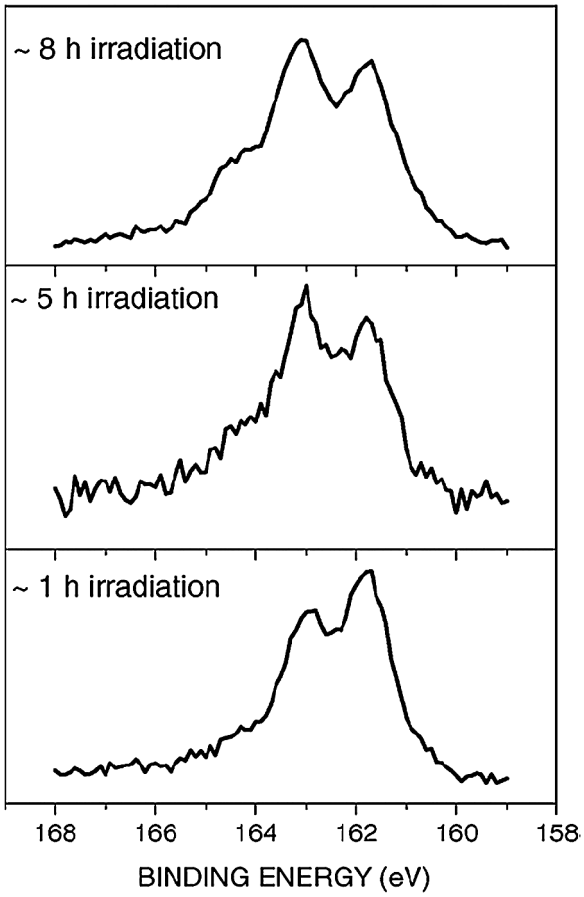


**Figure 15.** The S 2p XPS spectra measured from $Ag/C_{12}SH$ as a function of irradiation time using Mg Kα. The figure in Paper II is adapted.

In this work, four doublets were used to fit the high resolution S 2p spectra of the irradiated $Cu/C_{12}SH$ system (Figure 16). After an extended measurement time, the shape of the spectrum becomes so distorted that no individual peaks can be identified in the raw spectrum, which hampers the accurate determination of the BEs. However, a good fit can be obtained using four doublets with the S $2p_{3/2}$ BEs at ca. 161.9, 162.6, 163.2 and 163.8 eV. The S $2p_{3/2}$ signal at BE of 161.9 eV is connected with chemisorbed sulfur (S-Cu). The S $2p_{3/2}$ binding energy 162.6 eV can be attributed to thiolate $C_{12}S/Cu$. The BE at ca. 163.2 eV, observed in this work, can be assigned to irradiation damage. In addition, the component with BE of 163.8 eV was observed for both studied systems after a long irradiation time. It may be assigned to unbound disulfide but also with elemental sulfur.

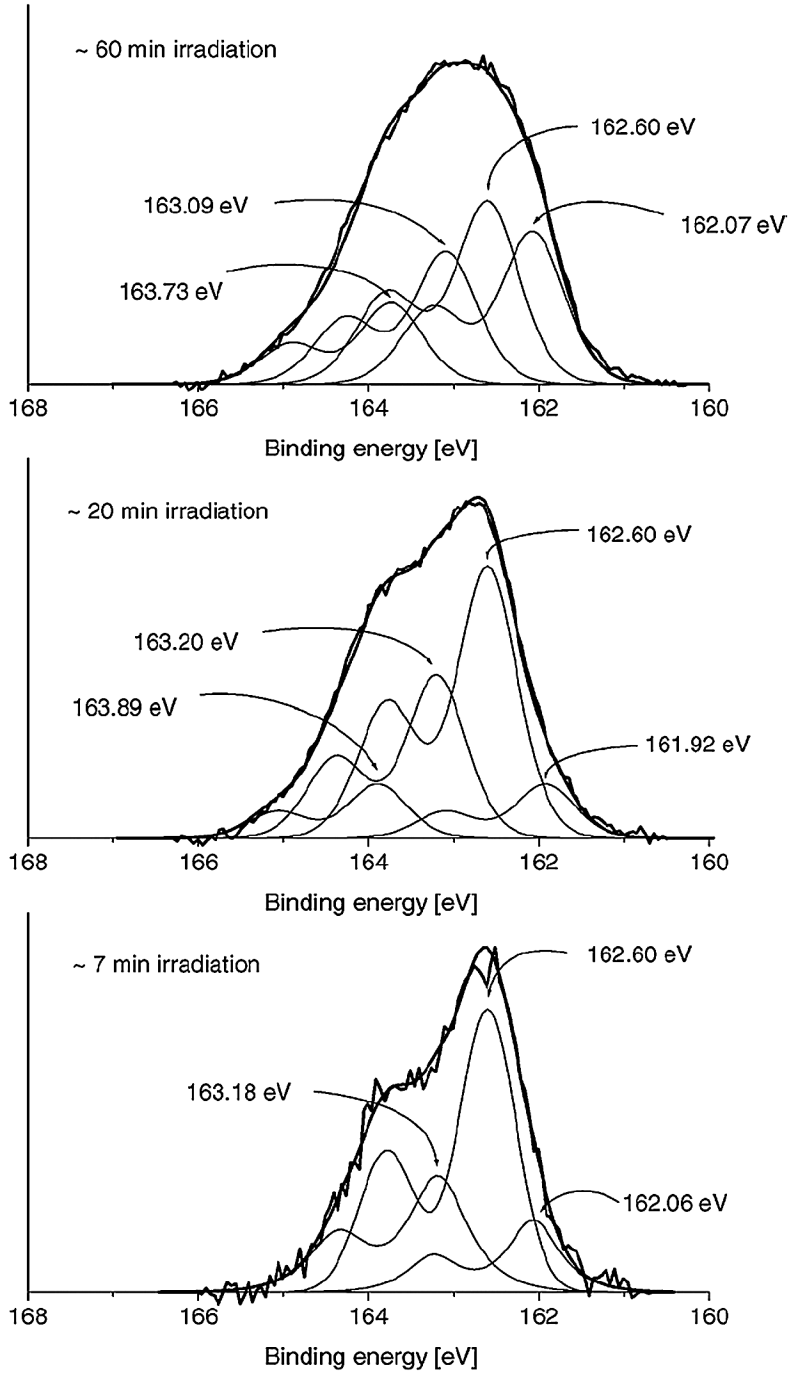


**Figure 16.** High-resolution (HR-XPS) spectra of S 2p emission line measured from $Cu/C_{12}SH$. Photon energy of 250 eV is used. The spectra are adapted from Paper II.

# 6.2. SAMs on Pt (paper III)

The self-assembled monolayers prepared from 1-dodecanethiol or S-dodecylthiosulfate have been characterized on polycrystalline gold and platinum surfaces. Additionally, a monocrystalline Pt(111) was also utilized in these studies.

Contact angle measurements and electrochemical impedance spectroscopy were performed to gain information on the quality of the layers. Alkyl thiol monolayers have a profound effect on the wetting of the electrode surface. The hydrophobicity of the surface is enhanced with increasing alkyl chain length and with pronounced film order. The static contact angles were measured for the four systems studied in this paper, Au/$C_{12}SH$, Au/$C_{12}SSO_3Na$, Pt/$C_{12}SH$, and Pt/$C_{12}SSO_3Na$ and are presented in Table 1. A general trend can be observed. Alkyl thiol SAMs exhibit larger contact angles than the thiosulfate monolayers on both Pt and Au and the layers on gold are more hydrophobic than the corresponding films on platinum. The impedance data were best accounted for by the modified Randles equivalent circuit, in which the interface consists of a charge transfer resistance $R_{ct}$ in series with a Warburg impedance $Z_W$, which are in parallel with a constant phase element (CPE). An effective capacitance value can be calculated from the fitted circuit parameters according to the method described by Brug et al., assuming the CPE behaviour to originate from the surface inhomogeneity.[89] The effective capacitances for the Au/$C_{12}SH$ and Pt/$C_{12}SH$ systems where identical (1.9 $\mu F\ cm^{-2}$) but the higher charge transfer resistance of the former (10.5 and 7 $k\Omega\ cm^2$, respectively) indicated better quality of the adsorbate layer. The capacitance of the Pt/$C_{12}SH$ interface is smaller than reported for the corresponding SAM of decanethiol on polycrystalline platinum, indicating that a better layer can be obtained with the longer aliphatic thiol.[90] The SAMs formed using Bunte salt exhibited greater variation in properties, especially in the $R_{ct}$ values. The effective capacitances for the Au/$C_{12}SSO_3Na$ and Pt/$C_{12}SSO_3Na$ interfaces were 2.0 and 2.8 $\mu F\ cm^{-2}$, respectively, and are presented in Table 1. These results indicate the same order of quality as observed in the contact angle experiments, i.e. on similarly treated substrates, the quality decreases in the order Au/$C_{12}SH$ > Pt/$C_{12}SH$ ~ Au/$C_{12}SSO_3Na$ > Pt/$C_{12}SSO_3Na$.

Table 1 : Static contact angles and effective capacitances of different SAMs

| *SAM* | *Au/$C_{12}SH$* | *Au/$C_{12}SSO_3Na$* | *Pt/$C_{12}SH$* | *Pt/$C_{12}SSO_3Na$* |
|---|---|---|---|---|
| Static contact angle | 101.7° | 100.8° | 101.2° | 100.5° |
| Effective capacitance | 1.9 μF $cm^{-2}$ | 2.0 μF $cm^{-2}$ | 1.9 μF $cm^{-2}$ | 2.8 μF $cm^{-2}$ |

XPS measurements show that the S–$SO_3$ bond of organic thiosulfates is broken in case of gold and platinum surfaces and the state of the surface-bound sulfur is indistinguishable from that of thiolate. In the S 2p XPS spectra of SAMs prepared from 1-dodecanethiol and S-dodecylthiosulfate, respectively, on polycrystalline platinum the only peaks appear around 163 eV with no signal at higher binding energies indicating that no oxygen containing sulfur species are present. In addition, the O 1s spectra displayed no traces of oxygen on the surface. Sodium was not detected, either.

The S 2p XPS spectrum (Al Kα excitation) of SAMs prepared from 1-dodecanethiol on polycrystalline platinum, S-dodecylthiosulfate on polycrystalline platinum, 1-dodecanethiol on Pt(111) and the HR-XPS spectrum (250 eV excitation) of SAM prepared from 1-dodecanethiol on polycrystalline platinum are presented in Figure 17. All of the S 2p spectra of SAMs on Pt show two closely spaced doublets at a binding energy of about 162.5 and 163.4 eV. In addition, a small third doublet was observed in high resolution XPS spectra at ca. 164 eV.

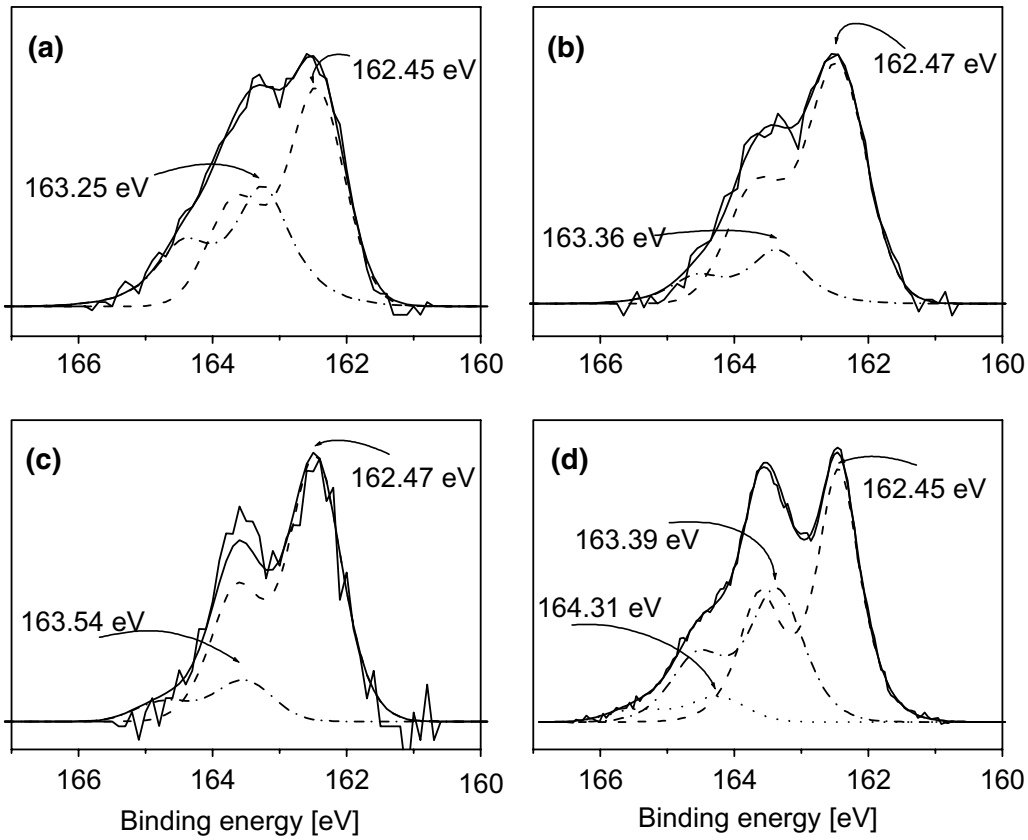


**Figure 17.** The S 2p XPS spectrum (Al Kα excitation) of SAMs prepared from (a) 1-dodecanethiol on polycrystalline platinum, (b) S-dodecylthiosulfate on polycrystalline platinum, (c) 1-dodecanethiol on Pt(111) and (d) HR-XPS spectrum (250 eV excitation) of SAM prepared from 1-dodecanethiol on polycrystalline platinum. The spectra are adapted from paper III.

On platinum, three sulfur species are formed upon SAM formation and we suggest that the catalytic activity of platinum is responsible for their existence in pristine monolayers. Although extrapolation from high vacuum conditions to the solution phase is not straightforward, we tentatively put forward the following mechanism for the origin of the new sulfur species on platinum surfaces (see Figure 18; only the hydrocarbon chains of surface-aligned thiols are shown and no attempt has been made to show bonding to platinum). Oxidative dehydrogenation, another well known process on platinum group metals,[91] can be ruled out because of the high temperature usually required and the absence of oxygen in our XPS spectra. During the first stage of the SAM formation the alkyl thiol molecules form a dense, flat surface-aligned phase.[92,93] The catalytically active platinum substrate interacts strongly with flat lying

molecules. The fragmentation of carbon chains may take place (upper level on Figure 18). Platinum partially dehydrogenates the adsorbed hydrocarbon chains forming hydrocarbon radicals and, possibly, adsorbed alkenes (second level on Figure 18). The thiols in solution effectively scavenge the radicals and produce thiyl radicals, which rapidly react with hydrocarbon radicals, alkenes or with each other (third level on Figure 18). Both surface reactions lead to the formation of dialkyl sulfides (lowest level in Figure 18), which have been identified as the species produced by X-ray irradiation in monolayers on gold.[23]

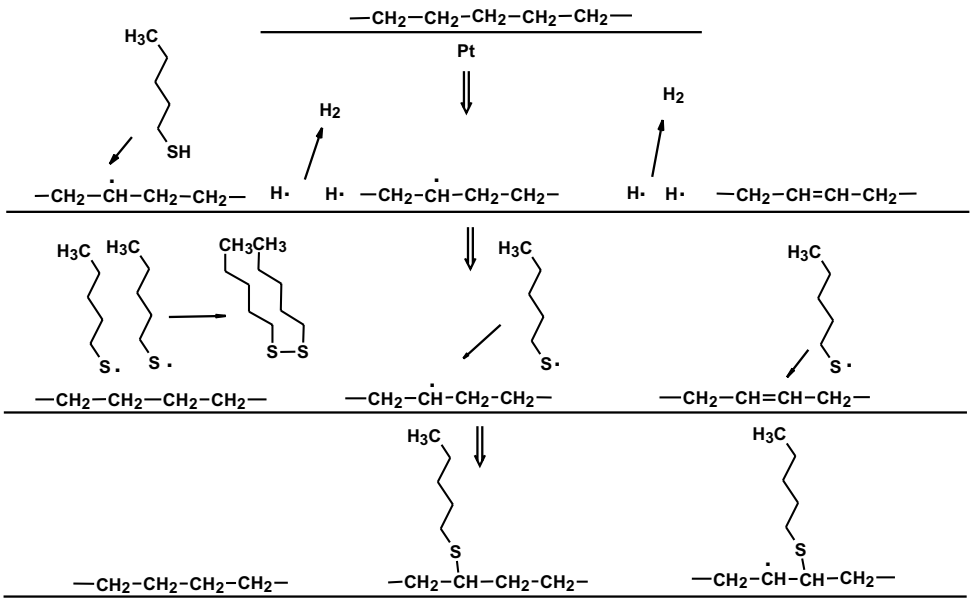


**Figure 18.** Schematic of possible mechanisms of dialkyl sulfide formation on platinum surface. The image is adapted from paper III.

# 6.3. Influence of surface oxygen on the formation of SAM (Paper IV)

In this study, monolayers were formed on clean and air-exposed metal substrates. The orientation of the individual molecules, structure and thereby characteristics of the ultrathin self-assembled monolayer are dependent on the substrate material: its structure and cleanliness. This study shows, the initial

oxygen contamination (originating from air) on the surface does not necessarily prevent formation of the tightly packed thiolate layer.

The first part of this study was concerned with the influence of thiol treatment on initially adsorbed air contamination. Reference samples were kept in air before thiol treatment. The chemical compositions of the surfaces before and after thiol treatment were compared using XPS. The changes in oxygen/metal ratios clearly indicate that oxygen has been removed from all of the studied surfaces after immersion of the sample into the thiol solution. Adsorbed oxygen is completely removed and replaced by thiol on the Au and Ag surfaces. Moreover, the change in the amount of oxygen on Pt surfaces is remarkable. On the copper surface, where an oxide layer is supposed to be formed on the surface during air exposure, some oxygen is still present after thiol treatment but its amount is diminished in this case, too.

The second part of the study is dealt with the influence of contamination on the formation of the thiol layer. We utilized comparative studies concerning the adsorption of thiol on the clean samples and initially air-treated samples to see how the surface contamination affects the formation of thiolate layer on a metal surface. Our results show that in the case of Au, Ag and Pt substrate materials the initial oxygen reduces adsorption of thiol on the surface. In contrast to the previously mentioned substrate materials, copper oxide seems to increase thiol adsorption.

In the third part of the study, the chemical shifts in XPS spectra measured from monolayers grown in 1 mM dodecanethiol in ethanol on air-contaminated and clean metal surfaces were reported and discussed. This section described the situation where oxygen has no effect on the shape of the XPS spectra of S 2p emission. The presence of initial oxygen on the metal surface before thiol treatment has no influence on the shape of Au 4f, Pt 4f, Ag 3d or Cu 2p spectra if they are measured after an adsorption of thiol. Similar spectrum shapes have been obtained from initially clean and initially air-contaminated surfaces. This means that oxygen does not take part in the final bonding of molecules to the surfaces. No oxidized sulfur species (S 2p BE > 166 eV)[51] such as sulfate or sulfide were detected by XPS on any of the samples.

The results obtained show that thiols remove contamination oxygen from gold, silver, platinum and copper surfaces, and tightly packed thiolate layers can be formed. The sulfur 2p XPS binding energies are not affected by initial oxygen, indicating that sulfur does not have any contact with the air-contaminated surface but rather it interacts with the clean metal.

# 6.4. ToF-SIMS study (Paper V)

In this study we investigated ToF-SIMS data of 1-dodecanethiol adsorbed on Au, Ag, Cu and Pt surfaces. One purpose of the studies was to extend our earlier analysis, (papers I and III) where we suggested dialkyl sulfide formation on the platinum surface during the dodecanethiol adsorption process.

ToF-SIMS is a rather sensitive surface analysis technique providing information on the chemical composition and molecular structure of SAMs. All the mass peaks from positive and negative ion spectra within the range $m/z$ = 0-2000 u are studied. Characteristic peaks associated with thiolate ions appear in the mass spectra. As can be suspected, a combination of organic, metal-organic and metal clusters are observed.

Even though ToF-SIMS is a chemical surface analysis technique, it can also give some information on the order of SAMs. In the spectra measured from the $Pt/C_{12}SH$ sample, the platinum peaks ($Pt^+$, $Pt_2^+$...) were accompanied with those associated to metal + hydrocarbon clusters, whereas the spectra obtained from $Au/C_{12}SH$, $Ag/C_{12}SH$ and $Cu/C_{12}SH$ revealed no prominent mass peaks on the higher mass side of the metal peaks, being consistent with the fragments of hydrocarbon chains. The situation can be seen in Figure 19. Indeed, this is the result concerning the order of the SAM. Metal + hydrocarbon fragments observed at the $Pt/C_{12}SH$ specimen are interpreted to originate from lying thiols that exist on the surface. Molecular fragments containing sulfur and parts of the hydrocarbon chain ($RS^-$) are detected. The existence of molecular ion clusters emitted from the surface is evidence of the formation of a thiolate layer. Large clusters like $Me_2[M\text{-}H]_3^-$ and $Me_3[M\text{-}H]_4^-$ can be seen in the negative ion spectra in cases where the bulk metal is Au, Ag or Cu. For the platinum specimen, very small peaks originating from large molecular clusters are seen.

ToF-SIMS data revealed that on gold, silver and copper substrates 1-dodecanethiol form dense standing-up phases, but on platinum, being a catalytically active substrate, we were also able to identify surface-aligned parallel lying molecules in addition to a standing thiolate layer. Our study shows that when ToF-SIMS spectra are analyzed, not only the existence of oligomers but also metal + hydrocarbon fragments give information about the order of SAM.

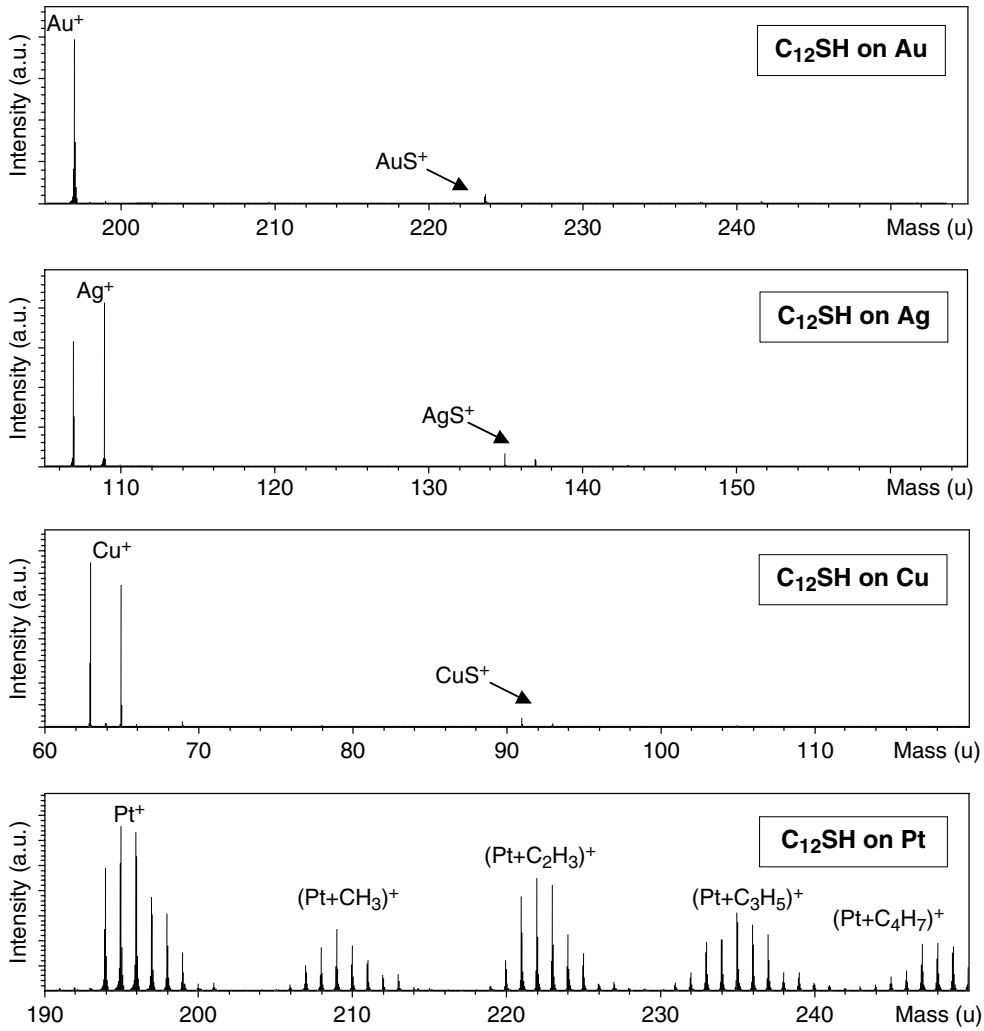


**Figure 19.** Positive ToF-SIMS spectra of $C_{12}SH$ treated Au, Ag, Cu and Pt surfaces. On the left hand side of each 60 amu wide spectrum window are metal ion peaks and on the higher *m/z* on the right hand side are metal + sulfur (*m/z* = 32) lines and those connected to metal + fragments of hydrocarbon chains. In the spectra measured from $Pt/C_{12}SH$ sample, the platinum peaks ($Pt^+$, $Pt_2^+$...) are accompanied with those associated with metal + hydrocarbon clusters, whereas the spectra measured from other substrates reveal no such components. The image is adapted from paper V.

# 7. Concluding remarks

Photoelectron spectroscopy was used as the main analysis method of these studies. XPS is a common method to characterize ordered molecular monolayers or multilayers, and it is routinely used for these purposes. Many studies have been published where it has been the main method for characterizing SAMs.[24,94,95,96] This method is surface sensitive because of the relatively small inelastic mean free path of the photoelectrons in a solid. It can be used to identify the chemical environment of the atoms. It is also possible to perform quantitative analysis with XPS by the measurement of peak intensities.

The presence of the monolayer is indicated by a large increase in the carbon and sulfur peak intensities, and a decrease in the metal peak intensities of the XPS survey spectra. The appearance of carbon and sulfur peaks is due to the existence of the surface layer. For all of the monolayers studied, we have observed the expected elements (those which can be attributed to substrate or adsorbate) and no others. A quantitative analysis of layers has been done based on the XPS measurements. The quality of the layers has been ascertained with contact angle measurements and electrochemical impedance spectroscopy.

Some of the measurements have been performed with synchrotron based photoelectron spectroscopy. The extreme surface sensitivity of synchrotron based measurements affects the intensity of signals from sulfur and metal. The energy region of the sulfur 2p emission line has been focused on during this study, as it can give much information on the sulfur/metal interaction. We have been able to see that sulfur was present in more than one kind of chemical environment even if there is only one sulfur atom in a thiol molecule. Identification of different sulfur species has been performed.

In spite of the fact that intentional and controlled modification of SAMs by electron interactions opens new possibilities for lithographic patterning to produce nanostructures it can also be considered as an undesirable side effect for an analytical technique such as XPS. We have been active in clarifying the influence of irradiation induced damage to the analysis. We have shown that the XPS method is suitable for this kind of analysis only if irradiation damage has been taken into account. In these studies, the conventional XPS measurements using non-monochromated X-ray source and synchrotron based HR-XPS have been done in order to study possible X-ray induced damage of thiolate films. The most noticeable processes were the loss of an orientational and conformational order, a partial dehydrogenation with the C=C double bond

formation, a desorption of film fragments, a reduction of the pristine thiolate species and the appearance of new sulfur species. An influence of these processes to the observed photoemission spectra has been elucidated.

The influence of exposing gold, silver, copper and platinum substrates to air prior to dodecanethiol deposition has been studied. The chemical composition of air includes several oxygen containing species. We have been able to show that the initial oxygen contamination (originating from air) on the surface does not prevent formation of the tightly packed thiolate layer. For all substrates the thiol deposition has been found partly or almost completely to reduce the oxide formed on the surface during an air exposure. These findings have relevance for applications.

Alkanethiolate SAMs at gold, silver, copper and platinum surfaces have been studied. The similarities and but also differences depending on surface materials have been observed. Dodecanethiol forms dense SAMs standing up from the surfaces for gold, silver and copper, while also molecules adsorbed parallel to the surface have been observed in the case of platinum. The XPS results for alkanethiolate on Pt reveal that the decomposition occurs upon deposition of the SAM, which is not further influenced by the radiation exposure during the XPS experiments. This difference on the interaction between SAMs and platinum surfaces has been studied in more detail. The differences have been interpretated due to the catalytic activity of platinum that affects to the self-assembly process.

# 8. Future challenges

This work on the adsorption of thiols started with studies on adsorption of sodium ethyl xanthate on pyrite. The studies continued with the investigations into adsorption of dodecanethiol on different metal substrates. The following ideas concerning future studies have occurred during the work.

- Would it be possible to produce an ordered SAM on Pt by potential control? A platinum sample could be installed into the potential cell and its surface potential could be manipulated before and during the insertion of thiol molecules to the solution.

- The assumption of the existence of short and midsize hydrocarbon fragments and metal-hydrocarbon species could be tested by analysing other samples that have not yet achieved complete SAM structures e.g. by following the relative intensity of these species as a function of the thiol adsorption time.

- It would be interesting to systematically test different substrate materials with 1-dodecanethiol. The substrates could be metals or other materials.

- Different molecules, such as aromatic thiols, could be studied in order to get information about the relationships between molecular structures and the resulting film structure and properties. Aromatic SAMs differ significantly from aliphatic ones in geometry, conformational degrees of freedom, and intermolecular interactions.[97]

- Different methods should be utilized in the studies. For example, surface NEXAFS studies in structure analysis especially for platinum substrate would give more information about the molecular structure on the surface.[98]

- The use of hard X-ray synchrotron radiation as the primary excitation for photoelectron spectroscopy has recently attracted great interest both worldwide and in our laboratory. The X-ray standing wave technique can be used for chemical depth profiling within layered structures of organic molecules which form self-assembled monolayers on surfaces such as thiols on coinage metals.[99]

# References

[1] Oudar, J.; Wise, H.: *Deactivation and poisoning of Catalysts* **1985**, Dekker, New York.

[2] Satterfield C.N. *Heterogenous Catalysis in Practice* **1980**, McGraw-Hill, New York.

[3] Ulman, A. *An Introduction to Ultrathin Organic Films: From Langmuir-Blodgett to Self-Assembly* **1991,** Academic Press, San Diego.

[4] Schreiber, F.; Eberhardt, A.; Leung, T. Y. B.; Schwartz, P.; Wetterer, S. M.; Lavrich, D. J.; Bermann, L.; Fenter, P.; Eisenberger, P.; Scoles, G. *Phys. Rev. B* **1998**, *57*, 12476-12481.

[5] Inoue, S; Sugiyama, S.; Travers, A. A.; Ohyama, T. *Biochemistry* **2007**, *46,* 164-171.
[6] Ulman, A. *Chem. Rev.* **1996**, *96*, 1533-1554.

[7] Xu, S.; Cruchon-Dupeyrat, S. J. N.; Garno, J. C.; Liu, G.-Y.; Jennings, G. K.; Yong, T.-H.; Laibinis, P. E. *J. Chem. Phys.* **1998,** *108*, 5002-5012.

[8] Schreiber, F. *Progress in Surf. Sci.* **2000**, *65*, 151-256.

[9] Eberhardt, A.; Fenter, P.; Eisenberger, P. *Surf. Sci.* **1998**, *397*, L285-L290.

[10] Kumar, A.; Whitesides, G. M. *Appl. Phys. Lett.* **1993**, *63*, 2002-2004.

[11] Kumar, A.; Biebuyck, H. A.; Whitesides, G. M. *Langmuir* **1994***, 10*, 1498-1511.

[12] Kühnle, A. *Curr Opin Colloid Interface Sci* **2008**, doi:10.1016/j.cocis.2008.01.001.

[13] Müller-Meskamp, L.; Lüssem, B.; Karthäuser, S.; Waser, R. *J. Phys. Chem. B* **2005**, *109*, 11424-11426.

[14] Tao, F.; Bernasek, S. L. *Chem. Rev.* **2007**, *107*, 1408-1453.

[15] Zanchet, D.; Moreno, M. S.; Ugarte, D. *Phys. Rev. Lett.* **1999**, *82*, 5277-5280.

[16] Rieley, H; Kendall, G. K. *Langmuir* **1999**, *15*, 8867-8875.

[17] Grönbeck, H.; Häkkinen, H. *J. Phys. Chem. B* **2007**, *111*, 3325-3327.

[18] Love, J. C.; Estroff, L. A.; Kriebel, J. K.; Nuzzo, R. G.; Whitesides, G. M. *Chem. Rev.* **2005**, *105*, 1103-1170.

[19] Laredo, T.; Leitch, J.; Chen, M.; Burgess, I. J.; Dutcher, J. R.; Lipkowski, J. *Langmuir* **2007**, *23*, 6205-6211.

[20] Mendoza, S. M.; Arfaoui, I.; Zanarini, S.; Paolucci, F.; Rudolf, P. *Langmuir* **2007**, *23,* 582-588.

[21] Petrovykh, D. Y.; Kimura-Suda, H.; Opdahl, A.; Richter, L. J.; Tarlov M. J.; Whitman, L. J. *Langmuir* **2006**, *22*, 2578-2587.

[22] Kato, H. S.; Noh, J.; Hara, M.; Kawai, M. *J. Phys. Chem. B* **2002**, *106*, 9655-9658.

[23] Heister, K.; Zharnikov, M.; Grunze, M.; Johansson, L. S. O.; Ulman, A. *Langmuir* **2001**, *17*, 8-11.

[24] Zerulla, D.; Chassé, T. *Langmuir* **1999**, *15*, 5285-5294.

[25] Chenakin, S. P.; Heinz, B.; Morgner, H. *Surf. Sci.* **1998**, *397*, 84-100.

[26] Wada, S.; Takigawa, M.; Matsushita, K.; Kizaki, H.; Tanaka, K. *Surf. Sci.* **2007**, *601*, 3833-3837.

[27] Ulman, A. *Thin Solid Films* **1996**, *273*, 48-53.

[28] Bain, C. D.; Troughton, E. B.; Tao, Y.-T.; Evall, J.; Whitesides, G. M.; Nuzzo, R. G. *J. Am. Chem. Soc.* **1989**, *111*, 321-335.

[29] Woods, R. *Flotation* **1976**, Furstenau, M.C., Ed., American Institute of Mining, Metallurgical, and Petroleum Engineers, Baltimore.

[30] Laajalehto, K.; Leppinen, J.; Kartio, I.; Laiho, T. *Colloids and Surfaces A: Physicochm. Eng. Aspects* **1999**, *154*, 193-199.

[31] Dulcey, C. S.; Georger, J. H.; Krauthamer, V.; Stenger, D. A.; Fare, T. L.; Calvert, J. M. *Science* **1991**, *252*, 551-554.

[32] Tiberio, R. C.; Craighead, H. G.; Lercel, C. M.; Lau, T; Sheen, C. W.; Allara, D. L. *Appl. Phys. Lett.* **1993**, *62*, 476-478.

[33] Williams, J. A.; Gorman, C. B. *Langmuir* **2007**, *23*, 3103-3105.

[34] Krämer, S.; Fuierer, R. R.; Gorman, C. B. *Chem. Rev.* **2003**, *103*, 4367-4418.

[35] Dong, X.-D.; Lu, J.; Cha, C. *Bioelectrochemistry and Bioenergetics* **1995**, *36*, 73-76.

[36] Castner, D. G.; Ratner, B. D. *Surf. Sci.* **2002**, *500*, 28-60.

[37] Nakano, K.; Yoshitake, T.; Yamashita, Y.; Bowden, E. F. *Langmuir* **2007**, *23*, 6270-6275.

[38] Zangmeister, R. A.; Maslar, J. E.; Opdahl, A.; Tarlov, M. J. *Langmuir* **2007**, *23*, 6252-6256.

[39] Brower, T. L.; Cook, M.; Ulman, A. *J. Phys. Chem. B* **2003**, *107*, 11721-11725.

[40] Salomäki, M.; Laiho, T.; Kankare, J. *Macromolecules* **2004**, *37*, 9585-9590.

[41] Lukkari, J.; Salomaki, M.; Ääritalo, T.; Loikas, K.; Laiho, T.; Kankare, J. *Langmuir* **2002**, *18*, 8496-8502.

[42] Viinikanoja, A.; Lukkari, J.; Ääritalo, T.; Laiho, T.; Kankare, J. *Langmuir* **2003**, *19*, 2768-2775.

[43] McGuiness, C. L.; Shaporenko, A.; Zharnikov, M.; Walker, A. V.; Allara, D. L. *J. Phys. Chem. C* **2007**, *111*, 4226-4234.

[44] Azzaroni, O.; Cipollone, M.; Vela, M. E.; Salvarezza, R. C. *Langmuir* **2001**, *17*, 1483-1487.

[45] Scherer, J.; Vogt, M. R.; Magnussen, O. M.; Behm, R. J. *Langmuir* **1997**, *13*, 7045-7051.

[46] Zamborini, F. P.; Crooks, R. M. *Langmuir* **1998**, *14*, 3279-3286.

[47] Briggs, D.; Seah M.P., Eds. *Practical surface analysis by Auger and X-ray Photoelectron Spectroscopy* **1983**, John Wiley & Sons, Chichester.

[48] Hüfner, S. *Photoelectron Spectroscopy Principles and Applications* **1995**, Springer-Verlag, Heidelberg.

[49] Lindgren, I. *J. Electron Spectrosc. Relat. Phenom.* **2004**, *137-140*, 59-71.

[50] Mårtensson, N.; Nilsson, A. *J. Electron Spectrosc. Relat. Phenom.* **1995**, *75*, 209-223.

[51] Lindberg, B. J.; Hamrin, K.; Johansson, G.; Gelius, U.; Fahlman, A.; Nordling, C.; Siegbahn, K. *Physica Scripta* **1970**, *1*, 286-298.

[52] Hernández-Laguna, A.; Maruani, J.; McWeeny, R.; Wilson, S., Eds., *Quantum Systems in Chemistry and Physics, Volume 2: Advanced Problems and Complex Systems* **2002,** Springer, Netherlands.

[53] Hesse, R.; Chassé, T.; Szargan, R. *Fresenius J. Anal. Chem.* **1999**, *365*, 48-54.

[54] Doniach, S.; Šunjić, M. *J. Phys. C* **1970**, *3*, 285-291.

[55] Jablonski, A.; Powell, C. J. *J. Electron Spectrosc. Relat. Phenom.* **1999**, *100*, 137-160.

[56] Jablonski, A. *Surf. Sci.* **1996**, *364*, 380-395.

[57] Seah, M. P.; Dench, W. A. *Surf. Interface Anal.* **1979,** *1*, 2-11.

[58] Powell, C. J.; Jablonski, A. *Surf. Interface Anal.* **2000**, *29*, 108-114.

[59] Powell, C.J. *J. Electron Spectrosc. Relat. Phenom.* **1988**, *47*, 197-214.

[60] Powell, C. J. *J. Electron Spectrosc. Relat. Phenom.* **1999**, *98-99*, 1-15.

[61] Margaritondo, G. *Introduction to Synchrotron Radiation* **1988**, Oxford University Press, Oxford.

[62] Schwinger, J. *Phys. Rev.* **1949**, *75*, 1912-1925.

[63] Andersen, J. N.; Johansson, U.; Nyholm, R.; Ullman, H., Eds., *Activity report 2003* **2004**, National Laboratory, Lund.

[64] Attwood, D. T., *Sychrotron Radiation for Material Science Applications* 2007, Electronic version (2008): http://www.coe.berkeley.edu/AST/sxreuv/

[65] Seah, M. P. *Surf. Interface Anal.* **1980**, *2*, 222-239.

[66] Nefedov, V. I. *J. Electron Spectrosc. Relat. Phenom.* **1999**, *100*, 1-15.

[67] Powell, C. J.; Jablonski, A.; Tanuma, S.; Penn, D. R. *J. Electron Spectrosc. Relat. Phenom.* **1994**, *68*, 605-616.

[68] Vickerman, J. C., Ed., *Surface Analysis - The Principal Techniques* **1997**, John Wiley & Sons Ltd, England.

[69] Vickerman, J.C.; Brown, A.; Reed, N.M., Eds., *Secondary Ion Mass Spectrometry, Principles and Applications* **1989**, Oxford University Press.

[70] Briggs, D.; Brown, A.; Vickerman, J.C. *Handbook of Static SIMS* **1989**, John Woley & Sons Ltd, Chichester and New York.

[71] product prochure: *PHI TRIFT V nano TOF Time-of-Flight SIMS* **2008**, Physical Electronics, Germany.

[72] Houssiau, L.; Bertrand, P. *Appl. Surf. Sci.* **2001**, *175-176*, 399-406.

[73] Peak, D. A.; Watkins, T. I. *J. Chem. Soc*. **1951**, 3292-3296.

[74] Svensson, S.; Forsell, J.-O.; Siegbahn, H.; Ausmees, A.; Bray, G.; Södergren, S.; Sundin, S.; Osborne, S. J.; Aksela, S.; Nõmmiste, E.; Jauhiainen, J.; Jurvansuu, M.; Karvonen, J.; Barta, P.; Salaneck, W. R.; Evaldsson, A.; Lögdlund, M.; Fahlman, A. *Rev. Sci. Instrum.* **1996**, *67*, 2149-2156.

[75] Mårtensson, N.; Baltzer, P.; Brühwiler, P.A.; Forsell, J.-O.; Nilsson, A.; Stenborg, A.; Wannberg, B. *J. Electron Spectrosc. Relat. Phenom.* **1994**, 70, 117-128.

[76] Boukamp, B. A. *Solid State Ionics* **1986**, *20*, 31-44.

[77] Zharnikov, M.; Frey, S.; Heister, K.; Grunze, M. *Langmuir* **2000**, *16*, 2697-2705.

[78] Heister, K.; Frey, S.; Gölzhäuser, A.; Ulman, A.; Zharnikov, M. J. Phys. Chem. B 1999, 103, 11098-11104.

[79] Kondoh, H.; Nozoye, H. *J. Phys. Chem. B* **1998**, *102*, 2367-2372.

[80] Meserole, C. A.; Vandeweert, E.; Chatterjee, R.; Winograd, N.; Postawa, Z. *Appl. Surf. Sci.* **1999**, *141*, 339-344.

[81] Yang, Y. W.; Fan, L. J. *Langmuir* **2002**, *18*, 1157-1164.

[82] Rodriguez, J. A.; Kuhn, M.; Hrbek, J. *J. Phys. Chem.* **1996**, *100*, 15494-15502.

[83] Rodriguez, J. A.; Kuhn, M.; Hrbek, J. *Chem. Phys. Lett.* **1996**, *251*, 13-19.

[84] Alonso, C.; Pascual, M. J.; Salomón, A. B.; Gutierrez, H. D.; López, M. F.; García-Alonso, M. C.; Escudero, M. L. *J. Electroanal. Chem.* **1997**, *435*, 241-254.

[85] Gutierrez, A.; Alonso, C.; López, M. F.; Escudero, M. L. *Surf. Sci.* **1999**, *430*, 206-212.

[86] Mullins, D. R.; Lyman, P. F. *J. Phys. Chem.* **1993**, *97*, 9226-9232.

[87] Mullins, D. R.; Lyman, P. F. *J. Phys. Chem.* **1993**, *97*, 12008-12013.

[88] Rufael, T. S.; Huntley, D. R.; Mullins, D. R.; Gland, J. L. *J. Phys. Chem.* **1995**, *99*, 11472.

[89] Brug, G. J.; van den Eeden, A. L. G.; Sluyters-Rehbach, M.; Sluyters, J. H. *J. Electroanal. Chem.* **1984**, *176*, 275-295.

[90] Lang, P.; Mekhalif, Z.; Rat, B.; Garnier, F. *J. Electroanal. Chem.* **1998**, *441*, 83-93.

[91] Huff, M.; Schmidt, L. D. *J. Phys. Chem.* **1993**, *97*, 11815-11822.

[92] Poirier, G. E. *Chem. Rev.* **1997**, *97*, 1117-1127.

[93] Poirier, G. E. *Langmuir* **1999**, *15*, 1167-1175.

[94] Ishida, T.; Hara, M.; Kojima, I.; Tsuneda, S.; Nishida, N.; Sasabe, H.; Knoll, W. *Langmuir* **1998**, *14*, 2092-2096.

[95] Whelan, C.M.; M.R. Smyth, C.J. Barnes, N.M.D. Brown, C.A. Anderson, Applied Surface Science 134 (1998) 144.

[96] Ang, T. P.; Wee, T. S. A.; Chin, W. S. *J. Phys. Chem. B* **2004**, *108*, 11001-11010.

[97] Cyganik, P.; Buck, M. *J. Am. Chem. Soc.* **2004**, *126*, 5960-5961.

[98] Kocharova, N.; Leiro, J.; Lukkari, J.; Heinonen, M.; Skala, T.; Sutara, F.; Skoda, M.; Vondracek, M. *Langmuir* **2008**, 24; 3235-3243.

[99] Drube, W. *Nuclear Instruments and Methods in Physics Research A* **2005**, *547*, 87–97